CleANN: Efficient Full Dynamism in Graph-based Approximate Nearest Neighbor Search

Ziyu Zhang
sylziyuz@csail.mit.edu
MIT CSAIL
USA

Yuanhao Wei
yuanhao1@mit.edu
MIT CSAIL
USA

Joshua Engels
jengels@mit.edu
MIT CSAIL
USA

Julian Shun
jshun@mit.edu
MIT CSAIL
USA

Abstract

Approximate nearest neighbor search (ANNS) has become a quintessential algorithmic problem for robotics, data mining, semantic search, unstructured data retrieval, and various other foundational data tasks for AI workloads. Graph-based ANNS indexes have superb empirical trade-offs in indexing cost, query efficiency, and query approximation quality. Most existing graph-based indexes are designed for the static scenario, where there are no updates to the data after the index is constructed. However, full dynamism (insertions, deletions, and searches) is crucial to providing up-to-date responses in applications using vector databases. It is desirable that the index efficiently supports updates and search queries concurrently. Existing dynamic graph-based indexes suffer from at least one of the following problems: (1) the query quality degrades as updates happen; and (2) the graph structure updates used to maintain the index quality upon updates are global and thus expensive.

To solve these problems, we propose the CleANN system which consists of three main components: (1) workload-aware linking of diverse search tree descendants to combat distribution shift; (2) query-adaptive on-the-fly neighborhood consolidation to efficiently handle deleted nodes; and (3) semi-lazy memory cleaning to clean up stale information in the data structure and reduce the work spent by the first two components. We evaluate CleANN on 7 diverse datasets on fully dynamic workloads and find that CleANN has query quality at least as good as if the index had been built statically using the corresponding data. In the in-memory setting using 56 hyper-threads, with all types of queries running concurrently, at the same recall level, CleANN achieves 7-1200x throughput improvement on million-scale real-world datasets. To the best of our knowledge, CleANN is the first concurrent ANNS index to achieve such efficiency while maintaining quality under full dynamism.

1 Introduction

Nearest neighbor search (NNS) is a well-studied problem with many applications where the relevance of data points can be captured by vector similarities, such as search engines [29], data clustering [6], and anomaly detection [43]. In these applications, datasets can be large and have several hundreds of dimensions and need to be searched quickly and accurately. The applications also frequently require multiple data points similar to the query, giving rise to the $k-$nearest neighbor search (KNNS) problem.

DEFINITION 1 (k-NEAREST NEIGHBORS (KNN)). *Given a dataset D with $|D| >> k$ in a space M with distance function $d(\cdot, \cdot)$, for a query $q \in M$, its k nearest neighbors $kNN(q)$ is a subset of D of size k satisfying $\forall x \in D \setminus kNN(q), \forall y \in kNN(q), d(y, q) < d(x, q)$.*

Indexes are designed to fulfill these search queries efficiently. Solving NNS or KNNS exactly in high dimensions is believed to be computationally hard [42], so researchers focus on the approximate nearest neighbor search problem (ANNS) instead. This problem has become increasingly important due to the ubiquity of vector embedding based semantic search for complex, multi-modal, unstructured data in AI applications [27].

Data are often constantly changing in many applications that need ANNS, such as recommendation systems [46], autonomous agents [36], and robotics [39]. Dynamism in ANNS is important for developing data systems that support efficient data updates and semantic search, which helps maintain content freshness and response to real-time inputs in AI applications. This motivates the need for a *dynamic* ANNS index that can keep up with, for example, the 500+ hours of content uploaded to YouTube [2] every minute, one billion images updated on JD.com every day [28], or the constant digestion of emails and code by an AI assistant. We are interested in the realistic *full dynamism* setting, where insertions, deletions, and searches can all happen concurrently.

Graph-based indexes such as VAMANA [20] (the in-memory version of DISKANN), HNSW [33], and NGT [19] have been shown [3, 34] to be state-of-the-art static ANNS algorithms (i.e., the index is not updated).[1] However, existing dynamic graph-based indexes [15, 45] suffer from at least one of the following problems: (1) the search quality may degrade as updates accumulate; and (2) the operations used to maintain the index quality upon updates are global and thus expensive. We present these problems in detail in subsection 1.1.

In this paper, we propose several techniques to address these issues. We propose *bridge building*, a data-aware method that improves the robustness of graph-based indexes. The key idea is to add additional edges between visited points that are moderately far apart during graph traversals. In addition, we propose a dynamic *neighborhood consolidation* method that identifies useful graph-structure updates around deleted points and performs these updates on the fly, without requiring any global batch operations that degrade system throughput. We also propose *semi-lazy cleaning*, a novel memory management strategy that efficiently cleans deleted nodes in the graph while maintaining graph quality, eliminating unnecessary neighborhood consolidation work. Finally, we present CleANN, an ANNS index that achieves efficient full dynamism using these techniques.

---

[1] The best performing systems evaluated in [3] are graph indexes with fine-grained optimizations such as quantization. These optimizations can be applied independently to the graph structure techniques that we focus on in this paper.

1.1 Limitations of Previous Work

1.1.1 Graph-based Indexes In a graph-based index $G = (V, E)$ for dataset $\mathbf{D}$, each node $v_x \in V$ represents a data point in $x \in \mathbf{D}$. Each graph-based index has its own algorithm for choosing how to connect edges between these nodes. Given a query point q, the index generally conducts a **best-first search (greedy search)** for q on G from a starting node s, i.e., the search repeatedly explores the node closest to q among unvisited neighbors in the search frontier. When the search converges (there are no nodes among the unvisited neighbors closer than the closest one among the visited nodes), the best visited nodes are reported as the approximate k-nearest neighbors, or **aKNN(q)**. In practice, the de-facto measure for the quality of **aKNN(q)** is the **recall**:[2]

DEFINITION 2 (RECALL K@K). *Given a dataset $\mathbf{D}$ and a query q, let $\mathbf{akNN}(q) \subseteq \mathbf{D}$ with $|\mathbf{akNN}(q)| = k$ be the result set returned by an ANN algorithm ALG. The recall k @ k of ALG for q is $\frac{1}{k}|\mathbf{kNN}(q) \cap \mathbf{akNN}(q)|$.*

Existing dynamic graph-based indexes [15, 45, 52] suffer from at least one of the following problems:

> **Deletion Efficiency Issue.** The operations that maintain the index quality upon updates are *global* and thus expensive.
>
> **Insertion Robustness Issue.** The search quality degrades as updates accumulate. The insertion algorithm is not robust with respect to the order in which the data points are inserted.

Deletion Efficiency Issue. When data points are deleted, **FRESH-VAMANA** [45] (the in-memory version of **FRESHDISKANN** and the state-of-the-art concurrent graph-based index capable of maintaining good query quality on million-scale real-world datasets) first marks the corresponding nodes as **tombstones** to filter them out in the responses for subsequent SEARCH queries. This approach requires periodically performing a global scan (known as *consolidation*) across the entire index to update edges and remove tombstones. The consolidation algorithm tries to connect all in-neighbors of each tombstone to all out-neighbors of the same tombstone, which incurs a significant cost. Furthermore, the search quality gradually decreases between these global consolidation steps as the index becomes stale. Our experiments show that the system throughput of **FRESHVAMANA** can decrease by more than 10x during consolidation but consolidation is required to achieve good SEARCH recalls (Figure 1).

LSH-APG uses the same approach of connecting all in-neighbors to all out-neighbors to fix the graph after a node is deleted, implying similar efficiency problems. **DEG** uses a global iterative optimization procedure to maintain the structure of the graph as nodes are inserted or deleted, incurring a significant cost, as shown in our experiments (Figure 21).

Insertion Robustness Issue. Graph-based ANN indexes are generally constructed by incrementally adding data points to the graph.
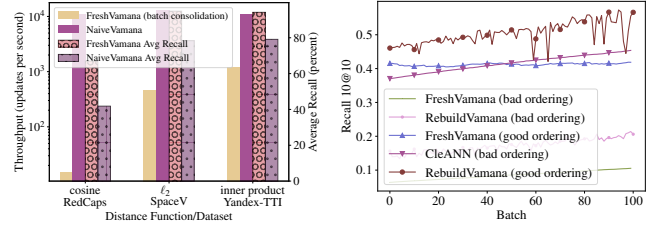

Figure 1: Search throughput and average recall with (FRESHVAMANA) or without (NAIVEVAMANA) concurrent global consolidation. The datasets are described in section 6.
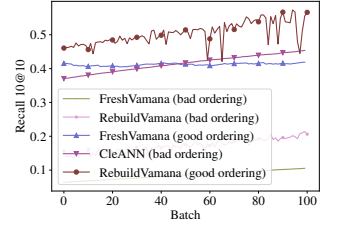

Figure 2: Synthetic dataset with a clustered distribution. A good ordering inserts whole clusters together and a bad ordering is uniformly random.

When a new data point $x_v \in \mathbf{D}$ is added, the index performs the following insertion routine:

> ROUTINE 1 (NEW DATA POINT INSERTION).
> (1) *Creates a node $v_x \in V$ to represent x.*
> (2) *Finds a set of candidate neighbor nodes C by conducting a best-first search for x.*
> (3) *Connects v_x with the nodes in C, and filters out edges according to some index-specific pruning algorithm.*

To construct an initial index, previous approaches combine Routine 1 with some global optimizations. For example, **HNSW** [33] imposes a global hierarchical structure over the candidate set C in step (2) and the edge choices in step (3); **FANNG** [14] runs global iterative optimizations after running Routine 1 on each data point; **LSH-APG** uses locality-sensitive hashing (LSH) to decide where the best-first search in step (2) starts; **VAMANA** processes the dataset with Routine 1 twice. While global optimizations help with robustness issues, they do not fully solve the problem. Naturally, practitioners use Routine 1 as an INSERT algorithm for indexes designed under the static setting like **HNSW**. The INSERT algorithms in dynamic indexes **LSH-APG** and **FRESHVAMANA** are also analogous to Routine 1. However, since the global optimizations mentioned above do not directly apply to dynamic settings, Routine 1 as an INSERT algorithm faces more robustness issues.

Intuitively, when v_x is inserted, the candidate set C only contains good neighbor candidates for v_x that are already present in the index. v_x may only be connected to a point v_y inserted after it if v_x is selected from the candidate set generated during the search in step (2) for v_y. Therefore, there may be good neighbors for v_x inserted after v_x that it never connects with. Without global optimizations during the initial index construction, Routine 1 as the INSERT algorithm is sensitive to the ordering in which points are inserted and therefore not *robust*.

In Figure 2, 1% of the dataset is inserted into the index on every batch. We run a test query batch after each insert batch, reporting the recall. **FRESHVAMANA**, which directly uses Routine 1 to insert data points, shows a large recall difference with different orderings. Compared to **REBUILDVAMANA**, which builds a **VAMANA** index from scratch every batch (and is a very inefficient algorithm for the dynamic setting), **FRESHVAMANA** has about a 10% lower recall under the same bad ordering, since it does not benefit from the global two-pass optimization of **REBUILDVAMANA**. These comparisons show that Routine 1 as an insertion algorithm is not robust.

---

[2]Usually "recall" means the proportion of correct data points returned, and "precision" means to the proportion of correct data points among the ones returned. The measurement of interest here incorporates both and is colloquially referred to as recall.

1.2 Our Contributions

In this paper, we present the **CleANN** system with three main techniques that address the limitations discussed in subsection 1.1.

(1) We propose *bridge building*, a data-aware algorithm that improves the robustness of dynamic graph-based indexes. The key idea is to add additional edges between visited points that are moderately far apart during an insertion. This helps address the insertion robustness issue and allows the algorithm to achieve good recall without needing a good ordering in the workload. In Figure 2, we see that **CleANN** with a bad insertion ordering has the same average recall as **FreshVamana** with a good ordering.

(2) We propose a dynamic *neighborhood consolidation* method that updates the graph around deleted points on the fly, without requiring any global operations that degrade query throughput. The graph update cost needed to actually delete a point is amortized across future operations.

(3) We propose *semi-lazy cleaning*, a novel memory management strategy that efficiently cleans deleted nodes in the graph while maintaining graph quality. The key idea is to stop the consolidation and recycle the deleted nodes early to reduce work. Together with dynamic neighborhood consolidation, this addresses the deletion efficiency issue, enabling the system to achieve both high update and search throughput and good recall.

Our techniques allow updates and queries to run concurrently. We evaluate **CleANN** on 7 diverse datasets. Our main experiments focus on the sliding window setting. A batch-based design is used to measure recall under dynamism and concurrency following previous work [20, 50]. Under this design, for each sliding window, we first issue an update batch that concurrently deletes old data points from the index and inserts new data points into the index. Then, a batch of search queries is run while the graph structure changes incurred by the updates continue to run concurrently in the background. We present corresponding efficiency results from the same sliding windows but with all three types of queries are run concurrently. We experimentally find that

(1) **CleANN** efficiently supports both Inserts and Deletes without requiring any expensive global operations or periodic rebuilds, achieving high throughput across different datasets and workload compositions.

(2) In the full dynamism setting, **CleANN** achieves the search quality of an index built from scratch with the corresponding data at a much lower cost. **CleANN** maintains high recall and is robust against different insertion orderings in the workload.

(3) **CleANN** scales well both in terms of dataset size and thread count.

In the in-memory setting using 56 hyper-threads, with updates running concurrently with searches, our searches are 7–1200x faster than that of **FreshVamana**, while maintaining similar query quality. Compared to the recent sequential baseline **DEG**, **CleANN** using a single thread is 1.2x and 3x faster for searches and updates, respectively. **CleANN** also scales better with dataset size compared to **DEG**. To our knowledge, **CleANN** is the first graph-based index to achieve such efficiency in a setting with full dynamism and concurrency.

Table 1: Notation for Parameters and Data Structures

Notation	Meaning
$d(p, q)$	Distance between nodes p and q
R	Graph out-degree bound
L	Beam width for beam search
L_I	Beam width for beam search during insertion
$N(v)$	Out-neighborhood of node v
$IN(v)$	In-neighborhood of node v
α	Sparsity heuristic parameter
$\pi(\cdot)$	Parent of node in a tree
C	Eagerness threshold

2 Preliminaries

2.1 Notation

In graph-based ANN indexes, each graph node corresponds to a data point. We use the letters q, x, y, and z to denote data points and u, v, and w to denote graph nodes. A subscript on a node (e.g., v_x) means that v_x represents the data point x. Uppercase letters in the script typeface (e.g., C, $\mathcal{N}$) represent sets of graph nodes or edges. Subscripts on algorithm names (e.g., GreedyBeamSearch$_L$) denote parameters for the algorithms. Algorithm-specific notation is listed in Table 1.

2.2 Background

In this subsection, we introduce the common algorithmic elements of graph-based ANN indexes and the technical details of **Vamana**, which our implementation of **CleANN** is based on.

2.2.1 Best-first Search and Backtracking The vanilla greedy search algorithm described in subsubsection 1.1.1 may converge at a local optimum. Therefore, ANN indexes commonly continue to explore a few close-to-optimal unvisited nodes in the frontier which helps escape the local optimum. This is referred to as **backtracking**. When the search terminates, the best k nodes among all visited nodes $\mathcal{V}$ are returned as the answer **aKNN**(q).

GreedyBeamSearch, shown in Algorithm 1, is the concrete best-first search algorithm in **Vamana**. GreedyBeamSearch uses a parameter L to control the scope of backtracking by terminating the search after finding L locally-optimal nodes. Line 4 initializes the frontier of the search with a set of pre-determined starting nodes. Line 5 keeps track of the L best nodes encountered, and is initialized with the starting nodes. Line 6 initializes the set of visited nodes $\mathcal{V}$ to be empty. Line 7 starts to visit a new node if at least one of the top L nodes closest to q ever encountered has not been visited. Line 8 chooses w, the closest node to q among the unvisited nodes in **frontier**. On Lines 9–15, the algorithm marks w as visited, removes it from the current frontier, adds all of its unexplored neighbors to the frontier, and updates $\mathcal{L}$ as needed.

2.2.2 Neighbor Candidate Selection and Pruning To help the best-first search efficiently find good approximate nearest neighbors, graph-based indexes carefully select edges to preserve in the graph. As discussed in Routine 1, when a new data point p is inserted, it is common to use the nodes visited during the best-first search for p as neighbor candidates for v_p, the new node representing p. Algorithm 2 describes the exact steps of Routine 1 in **Vamana** construction, and **FreshVamana** Insert. On Lines 4 and 5, Algorithm 2 uses the set of visited nodes $\mathcal{V}$ returned by GreedyBeamSearch

---

Algorithm 1 Greedy Beam Search (Algorithm 1 in [20])

1: L : Search beam width
2: **StartIds** : Starting nodes (can be fixed or computed beforehand)
3: **procedure** GREEDYBEAMSEARCH(q)
4:     frontier = {**StartIds**}
5:     $\mathcal{L}$ = {**StartIds**}   ▷ Maintains the L best nodes encountered
6:     $\mathcal{V} = \emptyset$ ▷ Visited nodes
7:     **while** frontier $\cap \mathcal{L} \neq \emptyset$ **do**
8:         $w = \mathrm{argmin}_{v_x \in \text{frontier} \cap \mathcal{L}} \, d(x, q)$
9:         $\mathcal{V} = \mathcal{V} \cup \{w\}$
10:        frontier = frontier $\setminus \{w\}$
11:        **for** $u \in N(w), u \notin \mathcal{V}$ **do**
12:           frontier = frontier $\cup \{u\}$
13:           **if** $d(u, q) < \max_{l \in \mathcal{L}} d(u, l)$ **then**
14:              $\mathcal{L} = \mathcal{L} \cup \{u\}$
15:              Delete $\mathrm{argmax}_{l \in \mathcal{L}} d(q, l)$ from $\mathcal{L}$.
16:     **return** $\mathcal{L}, \mathcal{V}$

Algorithm 2 Insert (Algorithm 3 in [20] and Algorithm 2 in [45])

1: L_I : Insertion beam width
2: **procedure** INSERT(p)
3:     Create graph node v_p to represent p.
4:     $\mathcal{L}, \mathcal{V} = $ GREEDYBEAMSEARCH$_{L_I}(p)$ (Algorithm 1)
5:     $N(v_p) = $ ROBUSTPRUNE($v_p, \mathcal{V}$) (Algorithm 3)
6:     **for** $w \in N(v_p)$ **do** ADDNEIGHBORS($w, \{v_p\}$) (Algorithm 5)

Algorithm 3 Robust Prune (Algorithm 2 in [20])

1: // C is the set of candidates
2: R : Global out-degree bound
3: α : Sparsity factor
4: **procedure** ROBUSTPRUNE(v, C)
5:     **if** $|C| \leq R$ **then**
6:         $N(v) \leftarrow C$
7:         **return**
8:     $\mathcal{N} = \emptyset$
9:     **while** $C \neq \emptyset$ **do**
10:        $p = \mathrm{argmin}_{c \in C} \, d(c, v)$. Remove p from C.
11:        $\mathcal{N} = \mathcal{N} \cup \{p\}$
12:        **for** $p' \in C$ **do**
13:           **if** $\alpha \cdot d(p', p) < d(p', v)$ **then**
14:              Remove p' from C
15:        **if** $|\mathcal{N}| \geq R$ **then break**

---

as the candidate set for neighbors of v_p in the pruning step (Step 3 in Routine 1). ROBUSTPRUNE (Algorithm 3) is the pruning algorithm used by **VAMANA**. Note that the algorithms that we propose in this work do not depend on the specifics of ROBUSTPRUNE.

3 Guided Bridge Building

In the static setting, previous works generally use a combination of the three steps in Routine 1 and global optimizations to construct a graph-based index. Most existing works [11, 14, 20, 32, 33, 45, 52] use the same insertion routine for post-construction insertions, including **FRESHVAMANA**, which we directly apply our algorithms to and compare with. As discussed in subsection 1.1, this insertion algorithm is not robust, exhibits search quality degradation compared to the static build.

Our algorithm GUIDEDBRIDGEBUILD addresses this issue by introducing new edges based on the nodes traversed in the best-first-search in an adaptive manner. We will see that guided bridge

building is critical to maintaining the quality of the index in the fully dynamic setting in the full benchmarks and ablation studies in section 6.

3.1 Setup and Idea

We explain GUIDEDBRIDGEBUILD under the context of **FRESHVAMANA**, which uses GREEDYBEAMSEARCH (Algorithm 1) with α-RNG heuristic edge pruning (Algorithm 3) under the framework of Algorithm 2 to implement INSERT. GUIDEDBRIDGEBUILD selectively adds edges among the nodes visited by GREEDYBEAMSEARCH. Our method is orthogonal to the α-RNG pruning and the GREEDYBEAMSEARCH backtracking method in **FRESHVAMANA** and may also be used to improve other graph-based indexes.

Let $\mathcal{V}$ be the set of nodes visited by the search phase of INSERT. $\mathcal{V}$ can be viewed as a search tree $\mathcal{T}$, where v is the parent of w (denoted as $v = \pi(w)$) if w was added to the search **frontier** during the exploration of v. To INSERT q, existing works [11, 33, 45] connect q to a subset of $\mathcal{V}$. **FRESHVAMANA** chooses this subset from $\mathcal{V}$ with ROBUSTPRUNE (Algorithm 3), which connects q with nodes close to it to improve search quality while promoting shortcut edges to improve efficiency.

Our key observation is that creating bridge edges among *cousins* in deeper levels (younger generations) of the search tree during a fully dynamic workload creates diverse paths that help with the robustness issue in INSERT, similar to what static ANN indexes achieve with global operations during the index construction phase. Deeper level cousins in the same search tree are likely to be nodes relatively close but not connected to each other via a short path. The lack of a direct connection can be caused by the robustness problem described in subsection 1.1. Without more direct connections, it takes a lot of backtracking for queries to navigate between them, resulting in longer convergence processes and possibly early pruning of the search, which leads to low search quality.

Thus, we propose GUIDEDBRIDGEBUILD, which introduces these missing connections. In addition to benefits in the dynamic case, we also find that GUIDEDBRIDGEBUILD can improve the recall of static ANN indexes by improving their robustness against bad orderings during the index construction phase.

To decide where to add bridge edges, GUIDEDBRIDGEBUILD runs an augmented GREEDYBEAMSEARCH, which we call BRIDGEBUILDERBEAMSEARCH (Algorithm 4). Lines 5–8 initialize the search frontier, the set of visited nodes, and the search tree $\mathcal{T}$. Each loop on Line 9 is a search step (Lines 10–14) exploring the best unexplored node w.

On Line 15, the algorithm marks unexplored out-neighbors of w added to the frontier in the current iteration as the children of w in the search tree $\mathcal{T}$. Line 16 invokes GUIDEDBRIDGEBUILD to add the bridge edges given $\mathcal{T}$ collected in BRIDGEBUILDERBEAMSEARCH. Nodes with search tree depths specified in $\mathcal{S}$ are tentatively bi-directionally connected. These connections are subject to additional heuristic constraints by HEURISTICPREDICATE. Lastly, Line 23 finalizes the bridge edges and performs additional local pruning if needed by calling Algorithm 5.

The sets $\mathcal{L}$ and $\mathcal{V}$ returned by BRIDGEBUILDERBEAMSEARCH on Line 17 can be used to either insert q as a new point (Algorithm 6) or to compute **aKNN**(q) by selecting the k nodes closest to q from

Algorithm 4 Guided Bridge Building

1: S : the set of layers considered
2: HEURISTICPREDICATE: function for imposing constraints on the bridge edges
3: $r(v) \equiv$ depth of v in $\mathcal{T}$
4: **procedure** BRIDGEBUILDERBEAMSEARCH(q)
5:    frontier = {**StartIds**}
6:    $\mathcal{V} = \emptyset$ // Visited nodes
7:    $\mathcal{T} = \{\pi(\textbf{StartIds}) = \textbf{null}\}$ // Search tree with only **StartIds**
8:    $\mathcal{L} \equiv$ best L ever seen in **frontier**.
9:    **while** frontier $\cap \mathcal{L} \neq \emptyset$ **do**
10:      $w = \text{argmin}_{v_x \in \textbf{frontier} \cap \mathcal{L}} \, d(x, q)$
11:      $\mathcal{V} = \mathcal{V} \cup \{w\}$
12:      frontier = frontier $\setminus w$
13:      **for** $u \in N(w), u \notin \mathcal{V}$ **do**
14:        frontier = frontier $\cup \{u\}$
15:        Record $w = \pi(u)$ in $\mathcal{T}$
16:    GUIDEDBRIDGEBUILD($\mathcal{T}$)
17:    **return** $\mathcal{L}, \mathcal{V}$
18: **procedure** GUIDEDBRIDGEBUILD($\mathcal{T}$)
19:    **for** $(v, w) \in \mathcal{T} \times \mathcal{T}$ such that $r(v) \in S$ and $r(w) \in S$ **do**
20:      $C = \emptyset$
21:      **if** HEURISTICPREDICATE(v, w) **then**
22:        $C = C \cup \{w\}$
23:      ADDNEIGHBORS(v, C) (Algorithm 5)

Algorithm 5 Add Neighbors

1: R : Global out-degree bound
2: **procedure** ADDNEIGHBORS(v, C)
3:    $\mathcal{N} = N(v) \cup C$
4:    **if** $|\mathcal{N}| < R$ **then** $N(v) = \mathcal{N}$
5:    **else** $N(v) = $ ROBUSTPRUNE($v, \mathcal{N}$) (Algorithm 3)

Algorithm 6 Robust Insert

1: L_I : Insert beam width
2: **procedure** ROBUSTINSERT(v_x)
3:    $\mathcal{L}, \mathcal{V} = $ BRIDGEBUILDERBEAMSEARCH$_{L=L_I}(v_x)$ (Algorithm 4)
4:    $N(v_x) = $ ROBUSTPRUNE($v_x, \mathcal{V}$) (Algorithm 3)
5:    **for** $w \in N(v)$ **do** ADDNEIGHBORS($w, \{v\}$) (Algorithm 5)
6: **procedure** ROBUSTINSERTDATA(x)
7:    Choose an empty or replaceable graph node to be the node v_x that represents x.
8:    ROBUSTINSERT(v_x)

$\mathcal{L}$. Therefore, GUIDEDBRIDGEBUILD can be used during INSERT or SEARCH queries.

3.1.1 Using GUIDEDBRIDGEBUILD in INSERT Algorithm 6 lists our insertion algorithm ROBUSTINSERT. Given a graph node v_x to insert, ROBUSTINSERT first performs BRIDGEBUILDERBEAMSEARCH for x. Then, ROBUSTPRUNE selects $N(v_x)$ from $\mathcal{V}$, the set of nodes visited during BRIDGEBUILDERBEAMSEARCH, and tries to add v_x to $N(w)$ for each $w \in N(v_x)$, using ROBUSTPRUNE as needed.

Example. Figure 3 illustrates ROBUSTINSERT with $L = 2$ and $R = 2$, with the exception that the degree constraint does not apply to the starting node s. $r(\cdot)$ is the depth in the search tree and $f(\cdot)$ is the order in which the nodes are explored. First, q is inserted. In Steps 1–2 (Subfigures 3a–3b), s, v_0, v_1, v_2, and u_2 are explored and added to $\mathcal{V}$. On Step 2, the search terminates with $L = 2$ and local minima of $d(\cdot, q)$: u_1 and u_2.

On Line 4 in Algorithm 6, ROBUSTINSERT selects a subset from $\mathcal{V}$ for q to connect to. ROBUSTINSERT uses the ROBUSTPRUNE procedure (Algorithm 3) from **VAMANA**. In Step 3 (Subfigure 3c), ROBUSTPRUNE selects u_1 as the first closest neighbor candidate (Line 10 of Algorithm 3), pruning out v_0 and v_2 (Line 14 in Algorithm 3). u_2 is subsequently selected as the next neighbor, reaching the out-degree bound $R = 2$. q is therefore connected to u_1 and u_2 (Subfigure 3d).

Next, GUIDEDBRIDGEBUILD with $S = \{1, 2\}$ and no HEURISTICPREDICATE considers edges at depth 1 and depth 2 of the search tree. The algorithm considers the edges $v_0 \leftrightarrow u_2$ and $u_1 \leftrightarrow v_2$. Subfigure 3e illustrates how u_1 causes the edge $v_0 \rightarrow u_2$ to be pruned. Similarly, v_2 causes the edge $u_2 \rightarrow v_0$ to be pruned. The edges $u_1 \leftrightarrow v_2$ are added as bridge edges (Subfigure 3f), concluding the insertion.

The example in Figure 3 also shows the algorithmic benefits of the bridge building algorithm. Subfigure 3g illustrates a search for $q^\star$ with the bridge edges present in the graph. The nodes s, v_2, u_1, and v_1 are explored in this order, correctly finding the nearest neighbor u_1. Subfigure 3h illustrates the search for $q^\star$ without bridge edges. s, v_2, and v_1 are explored, but the search terminates here, since v_1 and v_2 are local minima with respect to $d(\cdot, q^\star)$. v_0 which leads to u_1 is close to u_1 but too distant from the query compared to the other siblings of v_0. With a fixed backtracking budget, v_0 and u_1 are missed in the search. Therefore, the bridge edges between u_1 and v_2 improves the navigability of the graph.

3.1.2 Using GUIDEDBRIDGEBUILD in SEARCH A SEARCH query can also improve the part of the index that it traverses by using GUIDEDBRIDGEBUILD during the best-first search. Searching for other nearby points traverse similar parts of the graph and thus benefits from the improved navigability in these sectors. We hereby refer to SEARCH queries that perform GUIDEDBRIDGEBUILD *training* queries. In section 6, we find experimentally that training with a small number of in-distribution queries is sufficient for the index to adapt to distribution shifts in a query-aware fashion.

3.1.3 Hyperparameters S, and HEURISTICPREDICATE We found experimentally that $\Theta(\log(|\mathbf{D}|))$ is a good value range for S. HEURISTICPREDICATE further filters out candidate bridge edges to balance the cost of GUIDEDBRIDGEBUILD with the benefits of adding bridge edges. In our experiments, we set HEURISTICPREDICATE to require two endpoints of a bridge to have the same depth in $\mathcal{T}$.

3.1.4 Summary Our bridge building algorithm has 3 key benefits:
(1) Indexes whose construction and insertion use our algorithm have increased search quality compared to **FRESHVAMANA**.
(2) In a sliding window update scenario, our algorithm enables indexes to maintain quality at least as good as if the index were built from scratch with the corresponding data.
(3) Our method can effectively adapt to the update and query workload.

In addition, one can adapt GUIDEDBRIDGEBUILD to other graph-based indexes by modifying the beam search and using other pruning heuristics.

4 Dynamic Concurrent Data Structure Cleaning

In this section, we discuss how to handle DELETEs concurrently with INSERTs and SEARCHes. Due to the approximate nature of the
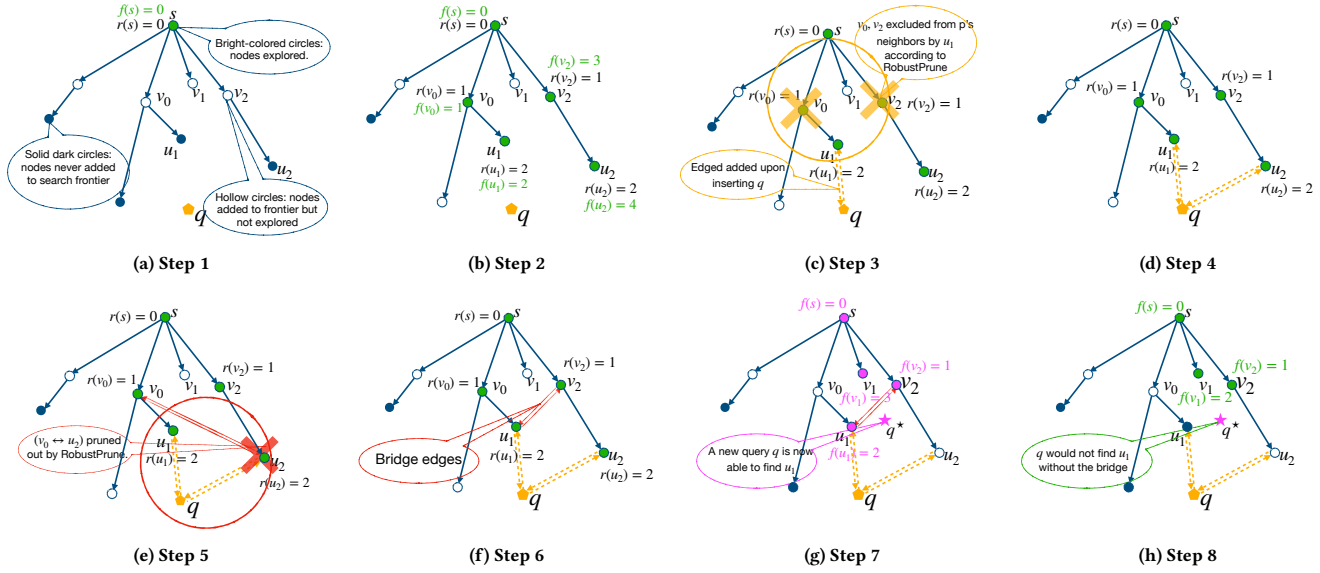
(a) Step 1 **(b) Step 2** **(c) Step 3** **(d) Step 4**

(e) Step 5 **(f) Step 6** **(g) Step 7** **(h) Step 8**

Figure 3: Step-by-step illustration of RobustInsert (Algorithm 6).

Algorithm 7 Consolidation (Subroutine of Algorithm 2 in [45])

1: R : Global out-degree bound
2: **procedure** Consolidate(v)
3:     $C = \emptyset$ // Neighbor Candidates
4:     **for** $w \in N(v)$ **do**
5:         **if** IsLive(w) **then**
6:             $C = C \cup \{w\}$
7:         **else** $C = C \cup \{u \neq v \wedge \text{IsLive}(u) \mid u \in N(w)\}$
8:     **if** $|C| < R$ **then** $N(v) = C$
9:     **else** $N(v) = \text{RobustPrune}(v, C)$

---

data structure and concurrent operations, there is no guarantee on when a newly inserted point will be correctly found by a subsequent Search. However, a user should not see a deleted point in the results of any Search queries executed after the Delete has completed. To achieve this consistency guarantee, it suffices to mark a deleted point as **tombstoned**, run any subsequent GreedyBeamSearches (Algorithm 1) normally, and leave out the tombstones when selecting the k best neighbors from $\mathcal{L}$. However, as the number of tombstones increases, the graph becomes contaminated, leading to a degradation in recall and efficiency, as observed by Xu et al. [50] and in our experiments. Therefore, to achieve high search quality, we need to remove the tombstones and update the graph accordingly.

The challenge of maintaining graph-based indexes while minimizing the number of tombstones lies in fixing graph edges of other nodes for which deleting the tombstones affects navigability. Previous graph-based ANN indexes use costly global operations to update the graph [15, 45, 52]. We propose adaptive dynamic techniques that address this challenge on the fly efficiently.

4.1 Algorithm Description

We say that a node is **live** if it is not a tombstone. Throughout the discussion, w_x is the tombstone node to be deleted. Concretely, the user called Delete on x earlier, the index has marked w_x as a tombstone, and the graph structure needs to be updated to reflect

the deletion of w_x. We base the discussion and implementation of our algorithm on Vamana, but our idea is applicable to any graph-based ANN index. The main idea of our algorithm is to perform neighborhood consolidation on the fly when needed.

Detecting Good Consolidation Targets On-the-fly. The best-first search algorithm (GreedyBeamSearch) can detect tombstone nodes used for navigation. During the traversals, if GreedyBeamSearch adds w_x to the search frontier when visiting v, i.e., $v = \pi(w_x)$ in $\mathcal{T}$, and v is live, then the edge $v \rightarrow w_x$ facilitated the $v \rightarrow w_x \rightarrow N(w_x)$ navigation. Therefore, it is useful to make v absorb $N(w_x)$ via neighborhood consolidation before we actually delete w_x. This can be carried out by either Insert or Search queries.

Consolidating all Tombstone Out-neighbors. Since all of $v's$ unexplored tombstone neighbors are added to the frontier at the same time during the beam search, it is cost-effective for v to consolidate with all of its tombstone neighbors' out-neighborhoods (Consolidate in Algorithm 7). This way, the tombstone nodes are processed more quickly, leading to a cleaner index.

Early Stopping of Consolidations. Intuitively, immediately removing w_x after only one in-neighbor v detects and consolidates with it does not preserve the navigability around w_x. However, waiting for all incoming neighbors of w_x to reach w_x through a GreedyBeamSearch and consolidate with w_x reduces to naively amortizing **FreshVamana**'s periodic consolidation of connecting all in-neighbors to all out-neighbors of a deleted node, which is computationally expensive.

Since our method chooses effective consolidation targets on-the-fly, we find that it is unnecessary to connect all $IN(w_x)$ to all $N(w_x)$, and that it suffices to visit a tombstone w_x just a few times with Consolidate(v) ($v = \pi(w_x)$ in some search tree $\mathcal{T}$) to preserve its navigation functionality. Therefore, we propose the following algorithm. We maintain a count for each tombstone of the number of times it has been visited by Consolidate from a live parent and stop performing more Consolidate's for w_x after
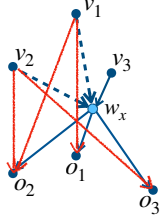
Figure 4: x is the data point being deleted (w_x is the corresponding node). Blue edges existed prior to the deletion. Red edges are added during CleanConsolidation. Solid edges exist after the consolidation finishes and w_x is marked as replaceable. Dashed edges are deleted.
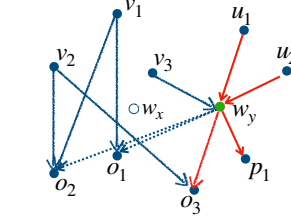
Figure 5: y replaces x to be the data point that w represents. Blue edges existed before the replacement. Red edges are determined using y. Solid edges exist after y is inserted and dashed edges are deleted as w_y's out-neighborhood is pruned using y.

the count hits an eagerness threshold C. We present an analysis on the sensitivity of C in subsubsection 6.3.5.

Semi-Lazy Cleaning. The remaining issue is to physically remove a tombstone node w_x from the graph after it has been processed by live parent nodes enough times with Consolidate. It may seem that we need to remove any dangling edge ($w_i \to w_x$) for each remaining $w_i \in IN(w_x)$ that has not consolidated with w_x. Maintaining and finding these w_i's and editing the out-neighborhood of each w_i would be expensive, as discussed in subsection 1.1.

We argue that cleaning the remaining dangling incoming edges is not necessary. The primary benefits of actually removing w_x and all of its *incoming* edges include (1) the storage for node w_x can be reused for future nodes that are inserted and (2) w_x's in-neighbors that did not call Consolidate on w_x's neighborhood do not unnecessarily explore w_x in future GreedyBeamSearches, which could make GreedyBeamSearches less likely to converge at the tombstone as a local optimum. Previous on-the-fly Consolidates for w_x already preserved most of the graph navigability around w_x. Therefore, we find that it is acceptable for a deleted point x to be overwritten by a *new data point* y, even when some of the in-neighbors previously still point to the old w_x node in the graph.

$N(w_x)$ and $IN(w_x)$ are formed by RobustInsert calls using x in its distance computations involving w_x. When a new data point y is inserted, if w_x has been processed by enough Consolidate calls, *we can turn w_x into w_y, letting the node represent y directly*. RobustInsert(w_y) uses y in its distance computations to obtain $N(w_y)$. Instead of actually creating a new node, $N(w_y)$ is merged into $N(w_x)$ and $IN(w_y)$ contains both new in-neighbors from RobustInsert(w_y) and the remaining $IN(w_x)$.

Moreover, the old incoming edges to w_x are present, but pointing to y instead of x. We call these edges **random edges**, where the randomness comes from the workload. We experimentally confirm (subsubsection 6.3.6) that these random edges do not significantly hurt the quality of the index, since GreedyBeamSearch naturally avoids exploring extremely far away nodes, and RobustPrune naturally removes edges that are less useful when the degree bound is exceeded. We call this technique **semi-lazy cleaning**.

Example. Figures 4 and 5 illustrate these algorithms. In this example, $C = 2$. In Figure 4, at the start, $N(w_x) = \{o_1, o_2, o_3\}$ and $IN(w_x) = \{v_1, v_2, v_3\}$. When x is deleted, w_x becomes a tombstone node. As queries explore v_1 and v_2 via GreedyBeamSearch, v_1 and v_2 consolidate with w_x, absorbing $\{o_1, o_2, o_3\}$ into $N(v_1)$ and

---

Algorithm 8 Clean Dynamic Beam Search

1: L : Search beam width.
2: **StartIds** : Fixed or separately computed nodes where the search starts
3: **H**: Global data structure for counting number of consolidations
4: C : Hyperparameter for consolidation
5: **performance_sensitive**: Flag for performance-sensitive queries
6: // For all w in the index, $\mathbf{H}(w) \geq 0$ if IsTombstoned(w) and w is not replaceable; otherwise $\mathbf{H}(w) = \mathbf{null}$.
7: **procedure** CleanDynamicBeamSearch(q, **performance_sensitive**)
8:   $\mathcal{T}$: Data structure for maintaining the search tree
9:   **frontier** = {**StartIds**}
10:   $\mathcal{L}$ = {**StartIds**} // Maintains the best L nodes encountered.
11:   $\mathcal{V} = \emptyset$ // Visited nodes
12:   **while frontier** $\cap \mathcal{L} \neq \emptyset$ **do**
13:     $w = \text{argmin}_{v \in \text{frontier} \cap \mathcal{L}}\, d(v, q)$
14:     $\mathcal{V} = \mathcal{V} \cup \{w\}$
15:     Remove w from **frontier**
16:     **if** IsTombstoned(w) $\wedge \mathbf{H}(w) \geq C$ **then**
17:       MarkReplaceable(w) // w is allowed to represent a new point.
18:       $\mathbf{H}(w) = \mathbf{null}$
19:     $\mathcal{N} = \{u \mid u \in N(w), u \notin \mathcal{V}\}$
20:     **for** $u \in \mathcal{N}$ **do**
21:       **frontier** = **frontier** $\cup \{u\}$
22:       **if** ¬**performance_sensitive** $\vee$ ¬IsTombstoned(u) **then**
23:         **if** $d(u, q) < \max_{l \in \mathcal{L}} d(u, l)$ **then**
24:           $\mathcal{L} = \mathcal{L} \cup \{u\}$
25:           Delete $\text{argmax}_{l \in \mathcal{L}}\, d(q, l)$ from $\mathcal{L}$ if $|\mathcal{L}| > L$
26:     Record $w = \pi(\mathcal{N})$ in $\mathcal{T}$
27:     **if** $\exists u \in \mathcal{N}$, IsTombstoned($u$) $\wedge$ ¬IsTombstoned(w) **then**
28:       CleanConsolidate(w) (Algorithm 9)
29:   **if** ¬**performance_sensitive** **then**
30:     GuidedBridgeBuild($\mathcal{T}$) (Algorithm 4)
31:   **return** $\mathcal{L}, \mathcal{V}$

Algorithm 9 Clean Consolidation

1: $\mathbf{H}$: Global data structure for counting number of consolidations
2: **procedure** CleanConsolidate(v)
3:   $\mathcal{N} = \{w \in N(v), \text{IsTombstoned}(w)\}$
4:   Consolidate(v)
5:   **for** $w \in \mathcal{N}$ **do**
6:     Increment $\mathbf{H}(w)$

Algorithm 10 CleANN Delete

1: $\mathbf{H}$: Global data structure for counting number of consolidations
2: **procedure** Delete(v)
3:   **if** $\mathbf{H}(v) \neq \mathbf{null}$ **then**
4:     $\mathbf{H}(v) = 0$

$N(v_2)$. The edges ($v_1 \to w_x$) and ($v_2 \to w_x$) are deleted. Since $C = 2$, v_2 does not perform CleanConsolidate anymore and the edge $v_3 \to w_x$ remains in the graph, and w becomes available for representing other data points.

In Figure 5, after y is inserted, w_x becomes w_y. $N(w_y)$ is formed with RobustInsert using the coordinates of y. During RobustPrune for w_y, both the old out-neighborhood $N(w_x)$ and the visited node set $\mathcal{V}$ generated by BridgeBuilderBeamSearch(y) are considered as candidates for $N(w_y)$. The random edge $v_3 \to w_y$ stays in the graph as well.

Algorithm. Algorithm 8 lists CleanDynamicBeamSearch, the full algorithm with on-the-fly consolidation and semi-lazy memory

---

Algorithm 11 CleANN Search

1: **procedure** SEARCH(k, q, **performance_sensitive**)
2:    $\mathcal{L}, _ = $ CLEANDYNAMICBEAMSEARCH(q, **performance_sensitive**)
3:    $\mathcal{L}' = \{v \in \mathcal{L} \mid \neg$IsTombStoned$(v)\}$
4:    **return** k best points in $\mathcal{L}'$ using brute force comparison with q

---

cleaning combined with the methods proposed in section 3. Apart from the bookkeeping for the best-first search and GUIDEDBRIDGE-BUILD, we now also need **H**, which helps maintain the tombstone information (Line 3). For all live nodes w, we have $\mathbf{H}(w) = $ **null**. For tombstoned nodes, **H** tracks the number of consolidations that have been performed for them.

During the best-first search, after the current best node w is selected to be explored and marked as visited (Lines 13–15), if w is a tombstone and has been consolidated for at least C times, w is marked replaceable (Line 16), and $\mathbf{H}(w)$ is set to **null**. On Lines 19–26, w is explored, adding its unvisited out-neighbors to the frontier and recording them as its children in the search tree $\mathcal{T}$. If any of these children are tombstoned nodes, the algorithm performs CLEANCONSOLIDATE(w) (Algorithm 9), consolidating the neighborhoods of all of w's deleted out-neighbors with w's neighborhood, incrementing **H** for the out-neighbors involved to record the consolidation, and pruning as appropriate (Lines 27–28).

For queries that are performance-sensitive, CLEANDYNAMICBEAM-SEARCH allows them to skip adding tombstone points to the search beam $\mathcal{L}$ (Line 22). In other words, the out-neighbors of tombstones will not be explored further, and the tombstone points do not count towards the L locally optimal points needed for the search to terminate. This optimization allow performance-sensitive queries take advantage of the consolidations that other queries already performed in this part of the graph by focusing on locally optimal nodes corresponding to live data points. Additionally, performance sensitive queries do not call GUIDEDBRIDGEBUILD. In our implementation, performance-sensitive queries still perform on-the-fly consolidation, as this computation is very cache-friendly.

4.2 Implementing Operations using CleanDynamicBeamSearch

Algorithm 11 lists the SEARCH query in **CleANN**. Similar to other graph-based indexes, it suffices to return the k best points in $\mathcal{L}$ generated by CLEANDYNAMICBEAMSEARCH. For DELETE, it suffices to mark the node deleted by toggling its **H** value from **null** to 0 (Algorithm 10). For INSERT, it suffices to substitute CLEANDYNAMICBEAMSEARCH for BRIDGEBUILDERBEAMSEARCH in ROBUSTINSERT (Algorithm 6).

5 Concurrency in CleANN

The algorithms that we propose can support the concurrent execution of SEARCH, INSERT, and DELETE queries. Data-level serializability is guaranteed, meaning that the insertion and deletion of data points always appear to have a serial ordering. The data structures that all queries synchronize over are the adjacency lists of the graph, the tombstone status tracker **H**, and a set keeping track of all empty slots available for new graph nodes (we refer to this as the set of replaceable nodes). Our implementation uses lock-based synchronization.

DELETE. Since DELETE only involves toggling **H** (Algorithm 10), DELETE(v) only needs to acquire an exclusive lock for $\mathbf{H}[v]$. Any concurrent SEARCH query that processes v during the final neighbor selection (Line 3 in Algorithm 11) after DELETE(v_x) will not include x in the result. After C consolidations have been performed for a deleted node v_x, we call MARKREPLACEABLE on the node (Line 17 in Algorithm 8), which inserts v into a set of replaceable nodes, making v available for representing a new data point. An exclusive lock over the set of replaceable nodes is held during MARKREPLACEABLE.

SEARCH. Following the concurrency techniques in **FRESHVAMANA**, When the graph is traversed, adjacency lists are protected by read-write locks (shared reader and exclusive writer). However, to prevent data loss or phantom data, i.e., INSERT(x) returns normally to the caller and DELETE(v_x) has not been called, but x appears to be not in the index, or vice versa, stricter synchronization on **H** is needed. For every v, once a CLEANDYNAMICBEAMSEARCH first explores v, it immediately acquires an exclusive lock for $\mathbf{H}(v)$ to check whether v should be marked replaceable (Line 17 in Algorithm 8). After acquiring the $\mathbf{H}(v)$ lock, if needed, the algorithm calls MARKREPLACEABLE over v.

GUIDEDBRIDGEBUILD does not introduce new synchronization on top of the locks for the adjacency lists as it only modifies the edges in the graph.

INSERT. The concurrency control in INSERT queries is mostly the same as for SEARCH except for two key differences. First, on Line 7 of ROBUSTINSERT (Algorithm 6), where when a graph node is chosen to represent the data point, the exclusive lock for the set of replaceable nodes is held. Together with the locking that happens in MARKREPLACEABLE, this ensures that data point additions and deletions are serialized. Second, when the adjacency lists of the new node and its neighbors are updated (Lines 4–5 of Algorithm 6), the corresponding exclusive locks of the adjacency lists are held.

6 Experiments

We study the performance of **CleANN**, which uses all of the methods from sections 3 and 4, and compare with existing solutions.

6.1 Experiment Setup

Sliding Window Batched Update. Each experiment consists of many rounds. On each round, we insert a batch of new data points and delete an equal number of the oldest data points. The numbers of the inserted and deleted points are 1% of the current index size. Real-world datasets are streamed in the order given to reflect realistic distribution shifts where applicable. At the end of each round, we issue all search queries in the dataset, and calculate the recall (Definition 2).

Since **GUIDEDBRIDGEBUILD** learns from queries, to avoid training and testing on the same queries, we issue a separate batch of in-distribution training queries generated by randomly sampling from test queries and adding a perturbation parameterized by the average nearest neighbor distance in the dataset before we issue the test queries. The size of the training query set is 2% of the test set (except for **RedCaps**, which uses 80 training queries). We designate only test queries as performance sensitive in Algorithm 8. When the search throughput is reported for this setting, we use

the weighted average for query throughput across training and test queries.

Sliding Window Batched Insert. This experiment setup is analogous to the Sliding Window Batched Update setting, except that no deletes are issued during the update batch on each round.

Sliding Window Mixed Update. This setting runs all types of queries concurrently. We issue INSERT, DELETE, training SEARCH, and test SEARCH queries concurrently. Recall is not measured in this experiment since the ground truth is not well-defined. To compare the recalls, we refer to the corresponding **Sliding Window Batched Update** experiments with the exact same data, sliding windows, and graph parameters.

Implementations. The implementation of **CleANN** is based on the open-source in-memory version of **DiskANN** (**Vamana**) [44]. We use a bit vector for maintaining nodes' tombstone statuses (instead of a hashset as used in **Vamana**) to enable efficient concurrent operations during cleaning. We use OpenMP for parallelism. We discuss the hyperparameters in **CleANN** in subsection 3.1.3. Our code is available at https://github.com/SylviaZiyuZhang/CleANN.

We compare with the following baselines:

- **RebuildVamana**: We build a static **Vamana** index from scratch using the two-pass build algorithm (with a uniformly random build order among the current points in the graph) with the corresponding data in the sliding window after each round and issue SEARCH queries on the static index. Rebuild costs are amortized onto the update and search workloads when presenting throughput results.

- **NaiveVamana**: We run **Vamana** with the base INSERT (Algorithm 2) and GREEDYBEAMSEARCH (Algorithm 1) algorithms. Deleted points are simply marked as tombstones and filtered out when the k nearest neighbors are selected from $\mathcal{L}$ as implemented in **FreshVamana**. Tombstones are never cleared from the graph.

- **FreshVamana**: We run **FreshVamana** [45], which uses Algorithm 2 for INSERTS and marks points as tombstones for DELETES. In the **Sliding Window Batched Update** setting, it performs global consolidation concurrently with the SEARCH batch. In the **Sliding Window Mixed Update** setting, global consolidation is concurrent with all types of operations.

- **DEG**: **DEG** [15] uses a continuous refinement routine to instantiate INSERTS and DELETES. The implementation currently available is sequential. Therefore, for each batch of updates, we first run the update queries, and then call the refinement routine. After the refinement routine finishes, we issue the SEARCH queries. We amortize the time taken for the refinement routine call of each batch onto the update and query workloads when reporting throughput results. We added cosine similarity to the implementation of **DEG**.

Hyperparameter Choices. We now revisit the hyperparameters required by the algorithms and discuss how they are set in the experiments. L configures the scope of SEARCH backtracking. L_I configures the scope of INSERT backtracking. R and α configure the sparsity of the graph via ROBUSTPRUNE. We vary these hyperparameters via parameter search for results shown in Table 3 and subsubsection 6.3.1. In the other experiments, we set $R = 64$, $\alpha = 1.2$, $L = 75$, and $L_I = 64$ following the conventional settings in previous

works [20, 34, 45]. $\mathcal{S}$ and HEURISTICPREDICATE configure **GuidedBridgeBuild**. Unless in one of the settings mentioned above requiring parameter search, we set $\mathcal{S} = \{\log_2 |\mathbf{D}| + 2, \log_2 |\mathbf{D}| + 3, \log_2 |\mathbf{D}| + 4\}$, and HEURISTICPREDICATE$(v_1, v_2) = \texttt{True}$ if and only if $r(v_1) = r(v_2)$ in the search tree $\mathcal{T}$ of BRIDGEBUILDERBEAMSEARCH.

C controls how eagerly the semi-lazy cleaning method completely cleans a tombstone. We set $C = 7$ except for in the experiments studying the sensitivity of the system to C in subsubsection 6.3.5.

Datasets. We use seven datasets for the evaluation, covering 3 distance functions (ℓ_2, inner-product, and cosine similarity) and different data distributions, with the numbers of dimensions ranging from 100 to 512. The datasets are listed in Table 2. **Sift** [3, 21] and **Glove** [3, 38] are long-standing benchmark datasets in ANNS corresponding to image and word representation, respectively. **MS-SpaceV** [7], **HuffPost** [17], and **RedCaps** [41] are real-world embedding-based information retrieval datasets with distribution shifts. We synthesized the **Adversarial** dataset by taking 10,000 uniform random seed samples from a hypercube and including Gaussian clusters of size 100 around the seed samples. **Adversarial**, **Yandex-tti**, and **RedCaps** have out-of-distribution search queries. For experiments where only a subset of a dataset was used, the subset is taken contiguously to preserve the distribution shift where applicable. An exception is **Yandex-tti**, where the full dataset has a real-world distribution shift; however, we use a sampled subset already provided by Yandex, which does not have a distribution shift.

Experiment Platform and Concurrency. All experiments are run on a 4-socket machine with a total of 112 Intel Xeon Platinum 8176 2.10 GHz CPUs with 2-way hyper-threading and 1.5TB DRAM. Unless otherwise specified, our algorithm and all variations of **Vamana** among the baselines use 96 hyper-threads during construction, and 56 hyper-threads without intra-query parallelism during query workloads.

6.2 Main Benchmark Results

We report the recall for $k = 50$ for all the main benchmark experiments. We summarize the recalls (under the Sliding Window Batched Update) and comparisons of the overall throughput results (under the Sliding Window Mixed Update setting) of **CleANN**, **FreshVamana**, and **RebuildVamana** in Table 3, running both experiment settings for 200 rounds.

We see that **CleANN** *achieves a recall competitive with **RebuildVamana** and **FreshVamana** while being much faster than both*. For datasets with a real-world distribution shift and/or out-of-distribution queries, **CleANN** outperforms **RebuildVamana** in terms of both recall and throughput on all but one datasets, suggesting that our algorithms can improve robustness.

6.2.1 Search Quality: Recall Figures 6–12 show the recalls of different variations on each dataset over 200 rounds in the Sliding Window Batched Update setting. Compared to **RebuildVamana**, **CleANN**'s recalls have similar average values but are more consistent across different rounds. **FreshVamana** has slightly higher recalls sometimes (at most 1–2% on average) since global consolidation, which exhaustively connects the neighborhoods of deleted

Table 2: Dataset Information.

Name	Full Size	#Queries	Dim.	Similarity	Distribution Shift	Domain	OOD Queries
Sift [3, 21]	1M	10,000	128	ℓ_2	No	Computer Vision	No
GloVe [3, 38]	1,183,514	10,000	100	cosine	No	Word Representation	No
MS-SpaceV [7]	1B	29,316	100	ℓ_2	Yes	Web Search	No
Yandex-tti [4]	1B	100,000	200	inner product	No	Text-to-Multimodal Search	Yes
RedCaps [41]	11.2M	800	512	cosine	Yes	Text-to-Multimodal Search	Yes
HuffPost [17]	200k	10,000	256	cosine	Yes	Short Text Representation	No
Adversarial	1.5M	10,000	128	ℓ_2	Yes	Synthetic Spatial	Yes

Table 3: Main Benchmark Result Summary. RV is REBUILDVAMANA and FV is FRESHVAMANA "× throughput" is multiplicative speedup of throughput (measured in the Sliding Window Mixed Update setting) of CLEANN compared to REBUILDVAMANA and FRESHVAMANA. $\alpha = 1.2$. Recall is 50@50. CLEANN uses $L = 75, L_i = 64$. REBUILDVAMANA and FRESHVAMANA use $L = L_i = 64$. Other parameters are varied to approximately match the recalls of different approaches.

Name	Size Used	#Queries	Update-Search Ratio	CLEANN | RV | FV recall	RV | FV × throughput
Sift [3]	150k	10,000	0.1	98.81% | 98.98% | 99%	15.17× | 7.73 ×
GloVe [3]	150k	10,000	0.1	87.14% | 87.07% | 87.68%	16.92× | 10.23×
MS-SpaceV [7]	1.5M	29,316	0.343	89.54% | 89.72% | 91.08%	35.82× | 7.88×
Yandex-tti [4]	1.5M	100,000	0.1	91.16% | 90.65% | 91.35%	13.04× | 3.69×
RedCaps [41]	1.5M	800	12.5	65.00% | 62.53% | 67.00%	343.6× | 1243.64×
HuffPost [17]	150k	10,000	0.1	95.35% | 95.24% | 95.57%	18.52× | 11.07×
Adversarial	1.5M	10,000	1	67.11% | 64.65% | 67.39%	15.55× | 25.21×

nodes, can create edges that are better for navigability. NAIVEVA-MANA suffers from recall degradation as more data are updated due to the graph becoming increasingly contaminated by tombstones. The experiments show that *CLEANN maintains high index quality when undergoing updates.*

6.2.2 Efficiency: Throughput
Figures 13–19 shows the throughput of different systems on each dataset with 56 hyper-threads in the Sliding Window Mixed Update setting. Compared to the baseline FRESHVAMANA, which maintains a similar recall as CLEANN (Figures 6–12) under the Sliding Window Batched Update setting with the same data and sliding windows, CLEANN has higher throughput across all datasets tested. The advantage of CLEANN is more pronounced as the workload becomes more write-intensive.

NAIVEVAMANA has higher throughput compared to CLEANN but suffers from severe and fundamental recall degradation (see Figures 6–12). Since REBUILDVAMANA does not support concurrent search and updates, we report the search throughput with the build cost amortized onto the workload. This adjusted throughput of REBUILDVAMANA is significantly lower than CLEANN due to the costs of building the index from scratch.

6.2.3 Comparison with Sequential Baseline
We compare CLEANN using one thread with the sequential baseline **DEG** in the Sliding Window Batched Update scenario. We used a machine with Intel Xeon CPU E5-2699 2.2GHz CPUs with 64GB RAM for this experiment. We use $\varepsilon = 0.03$ for **DEG** and $L = 64$ for CLEANN to align the recall of the two systems (Figure 20), allowing for a direct comparison. Figure 21 shows that CLEANN has approximately $4x$ INSERT throughput and $1.5x$ SEARCH throughput on **RedCaps** (with an index of size 500,000) compared to **DEG**. This further suggests that our method is more efficient compared to **DEG**'s global optimization method—such global operations are expensive as discussed in section 4.

6.3 Trade-off, Scalability, and Ablation Studies

6.3.1 Trade-offs between Search/Update Throughputs and Search Quality
Figures 22–33 show the tradeoffs between search and update throughputs and recalls on each dataset at round 100 measured in the Sliding Window Batched Update setting. In this setting, the graph structure updates of the FRESHVAMANA global consolidation run concurrently with the search queries. For some datasets, FRESHVAMANA only has one data point due to the high computational resources needed to run the workload on FRESHVAMANA. We chose not to run the global consolidation concurrently with update queries as the consolidation would only be able to fix the graph based on previous update batches and not the current one. NAIVEVAMANA and CLEANN are searched on the same set of hyperparameters ($1 \leq \alpha \leq 1.3$ and $64 \leq L \leq 128$, $\mathcal{S} = \{[3, 4, 5], \ldots, [\log_2 |\mathbf{D}| + 2, \log_2 |\mathbf{D}| + 3, \log_2 |\mathbf{D}| + 4]\}$). For FRESHVAMANA, $\alpha = 1.2, L_I = L = 64$.

Across all datasets, CLEANN is the only method achieving both good search throughput and high recall, filling the upper-right corner of the trade-off plots. In particular, NAIVEVAMANA struggles to reach the high recall region, and FRESHVAMANA has at least an order of magnitude lower search throughput. Compared to FRESHVAMANA, CLEANN has 25–60% lower update throughput. This is because part of the graph structure update costs are not included in the update throughput measurement for FRESHVAMANA. This difference in the update throughput is in fact the overhead of supporting dynamism of CLEANN compared to using a naive INSERT (Algorithm 2) and DELETE (simply marking deleted points as tombstones). However, the overall throughput of CLEANN is higher than FRESHVAMANA as discussed in subsection 6.2. These results suggest that *CLEANN efficiently achieves full dynamism, reaching a good overall trade-off on search cost, update cost, and query quality.*

6.3.2 Parallelism Scalability
We study the scalability of CLEANN in the Sliding Window Batched Update experiment for 100 rounds on **MS-SpaceV** with an initial index size of 5 million using 1–224

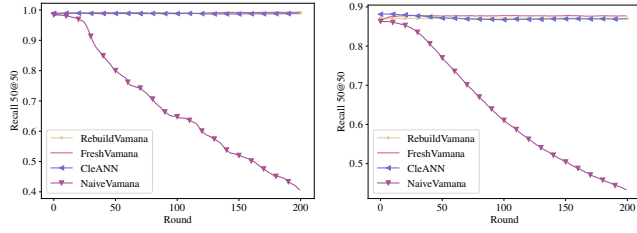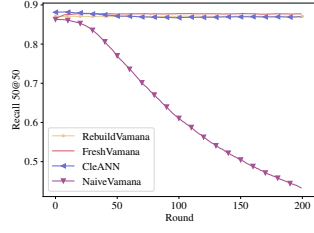**Figure 6: Recall over updates for Sift with index size 50k.**

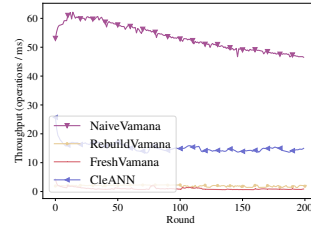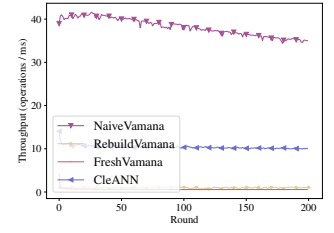

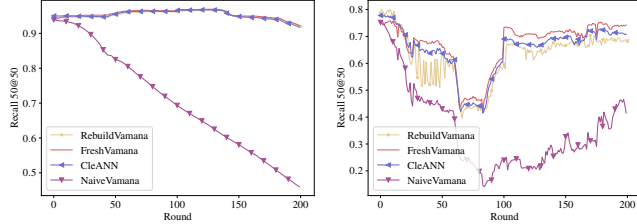**Figure 7: Recall over updates for GloVe with index size 50k.**

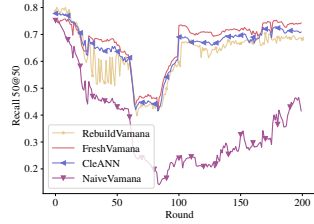**Figure 8: Recall over updates for Huff-Post with index size 50k.**

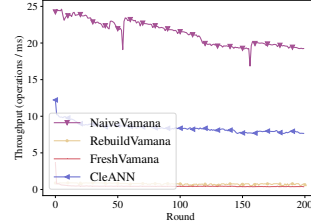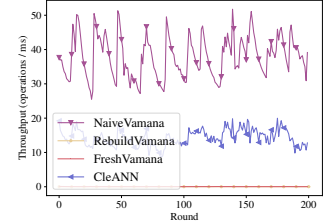**Figure 9: Recall over updates for Red-Caps with index size 500k.**
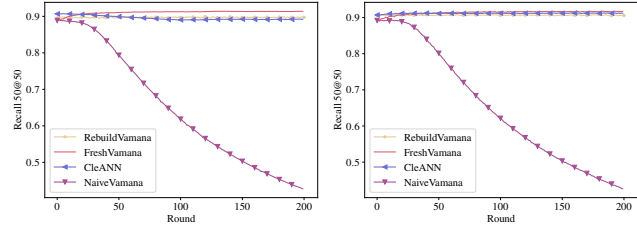

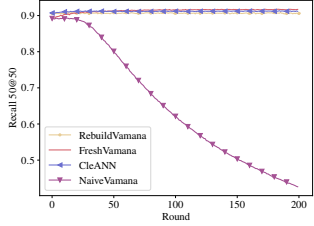**Figure 10: Recall over updates for SpaceV with index size 500k.**

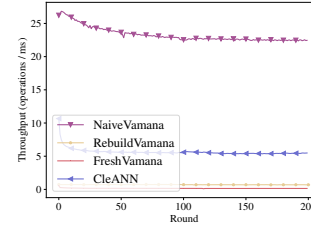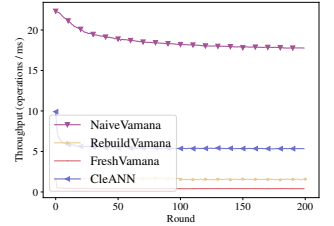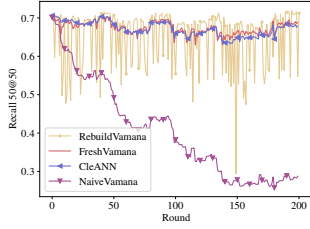**Figure 11: Recall over updates for Yandex-tti with index size 500k.**

Figure 12: Recall over updates for Adversarial with index size 50k.

Figure 13: Throughput over updates for Sift with index size 50k.

Figure 14: Throughput over updates for GloVe with index size 50k.

Figure 15: Throughput over updates for HuffPost with index size 50k.

Figure 16: Throughput over updates for RedCaps with index size 500k.

Figure 17: Throughput over updates for SpaceV with index size 500k.

Figure 18: Throughput over updates for Yandex-tti with index size 500k.

Figure 19: Throughput for Adversarial with index size 50k.

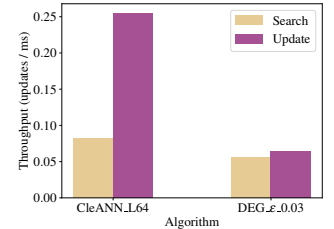**Figure 20: Recall on RedCaps with an index of size 500,000 of CleANN, FreshVamana, and DEG with $\varepsilon = 0.03$.**

Figure 21: Single-thread throughput on RedCaps with an index of size 500,000 of CleANN, and DEG with $\varepsilon = 0.03$.

hyper-threads. These results are shown in Figure 34. Compared to the single-threaded performance, the Search/Insert throughputs are 2x with 2 threads, 6.5x/6.8x at 8 threads, 17.45x/19.75x at 28 threads, and 34.96x/43.74x at 112 threads. The scaling slows down and eventually slightly degrades as more hyper-threads are used, as the number of operations becomes insufficient to saturate all of the hyper-threads and the contentions on global locks become more severe. These findings are consistent with previous results [34] on **Vamana**. **CleANN** maintains at least 90% recall throughout this experiment.

*6.3.3 Ablation study for **GuidedBridgeBuild*** In this section, we study the individual effects of **GuidedBridgeBuild** through three experiments. All experiments are performed with the same parameters: $L = L_i = 64$, $\alpha = 1.2$, and $R = 64$.

Sliding Window Batched Insert. We use the **Adversarial** synthetic dataset, shuffle it, start with an index of size 500,000 and run the experiment for 100 rounds. We compare the recall between

when the index construction and Inserts use **GuidedBridge-Build** versus **FreshVamana**. The training batches use 2% of the test queries. Figure 35 shows that **GuidedBridgeBuild** gives over 30% higher recalls compared to **FreshVamana** and
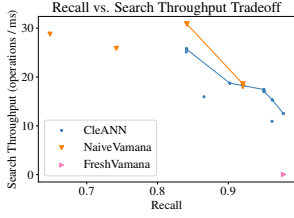
Figure 22: Tradeoff between average search throughput and recall at round 100 on Sift with index size 50k. (Higher and to the right is better.)
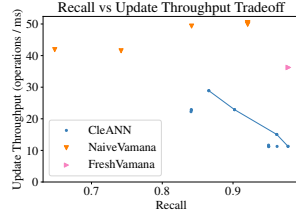
Figure 23: Tradeoff between average update throughput and recall at round 100 on RedCaps with index size 500k. (Higher and to the right is better.)
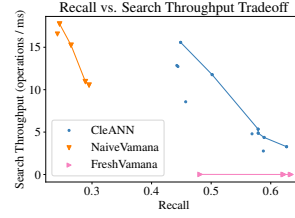
Figure 28: Tradeoff between average search throughput and recall at round 100 on RedCaps with index size 500k. (Higher and to the right is better.)
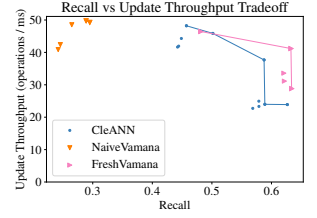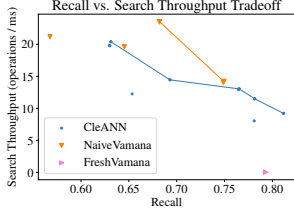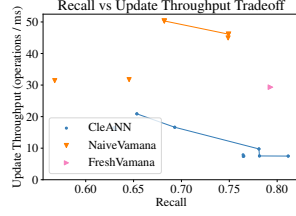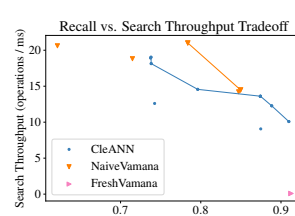
Figure 29: Tradeoff and optimal frontier between average update throughput and recall at round 100 on RedCaps with index size 500k. (Higher and to the right is better.)

Figure 24: Tradeoff between average search throughput and recall at round 100 on RedCaps with index size 500k. (Higher and to the right is better.)

Figure 25: Tradeoff and optimal frontier between average update throughput and recall at round 100 on GloVe with index size 50k. (Higher and to the right is better.)

Figure 30: Tradeoff between average search throughput and recall at round 100 on SpaceV with index size 500k. (Higher and to the right is better.)
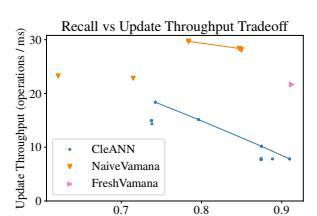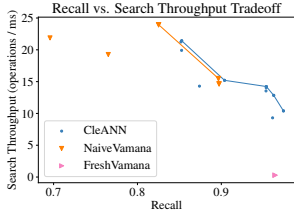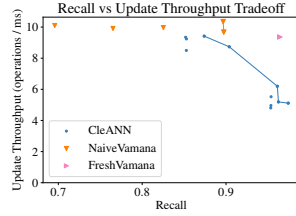
Figure 31: Tradeoff and optimal frontier between average update throughput and recall at round 100 on SpaceV with index size 500k. (Higher and to the right is better.)

Figure 26: Tradeoff between average search throughput and recall at round 100 on HuffPost with index size 50k. (Higher and to the right is better.)

Figure 27: Tradeoff and optimal frontier between average update throughput and recall at round 100 on RedCaps with index size 500k. (Higher and to the right is better.)
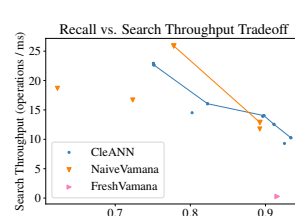
Figure 32: Tradeoff between average search throughput and recall at round 100 on Yandex-tti with index size 500k. (Higher and to the right is better.)
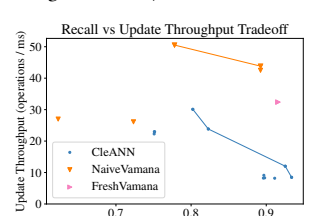
Figure 33: Tradeoff and optimal frontier between average update throughput and recall at round 100 on Yandex-tti with index size 500k. (Higher and to the right is better.)

20% higher compared to **RebuildVamana** on the same graph parameters, clearly indicating that **GuidedBridgeBuild** improves the index quality.

Sliding Window Batched Update. We now study **GuidedBridge-Build** in the Sliding Window Batched Update setting, where we have **Delete** queries and tombstone nodes. We run the experiment for 100 rounds and maintain an index of size 500,000 using the **RedCaps** dataset. This experiment does not use the training phase of the standard Sliding Window Batched Update experiment as we will study **Search**-based training separately.

We compare the recall from the search batches when the build and **Insert** processes use **GuidedBridgeBuild** versus **NaiveVamana** and **RebuildVamana**. Figure 36 shows that **GuidedBridgeBuild** improves recall by 6–7% over **NaiveVamana**. **RebuildVamana** has up to 15% lower recall compared to **GuidedBridgeBuild** for the earlier batches. However, **RebuildVamana** has significantly better recall for the later batches since it does not have tombstones saturating the search beam, while **GuidedBridgeBuild** and **NaiveVamana** do. **RedCaps** has both real-world distribution shift and out-of-distribution queries. This
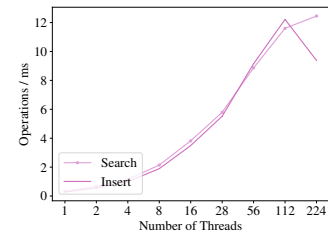

Figure 34: Update and Search throughput of MS-SpaceV under Sliding Window Batched Update with index size 5 million points using different numbers of threads.

experiment shows that the adaptive graph improvement provided by **GuidedBridgeBuild** helps address these challenges.

Query Awareness. As discussed earlier, GuidedBridgeBuild can be used by **Search** queries to improve the navigability of the area of the graph that they traverse, giving the index the ability to learn from queries and improve in the frequently traversed areas with limited complexity budget. We demonstrate this ability by training with in-distribution and out-of-distribution queries in the Sliding Window Batched Update setting on **MS-SpaceV** and **RedCaps** and
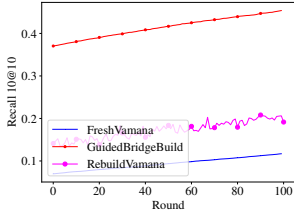
Figure 35: Recall 10@10 with and without GuidedBridgeBuild when starting with an index of size 500,000 of the Adversarial dataset in the Sliding Window Batched Insert setting. GuidedBridgeBuild uses $S = [2, \ldots, 12]$.
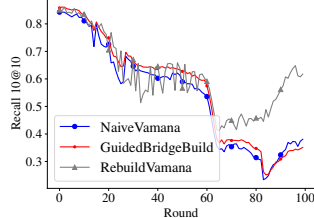
Figure 36: Recall 10@10 with and without GuidedBridgeBuild for inserts on RedCaps over a sliding window of 500,000 points.

Figure 39: Recall 50@50 over a sliding window of 500,000 MS-SpaceV points. NaiveVamana uses the FreshVamana tombstone scheme w/o consolidations.

Figure 40: Overall throughput in Sliding Window Mixed Update over a sliding window of 500,000 MS-SpaceV points. The lines for RebuildVamana and FreshVamana are overlapping.
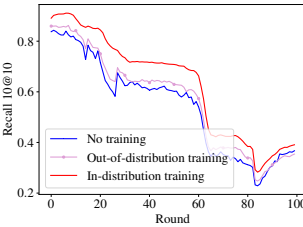
Figure 37: Recall 10@10 on RedCaps for different variations of using training queries.
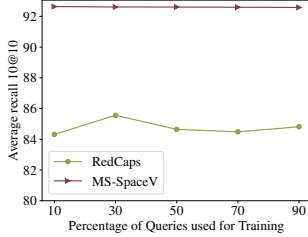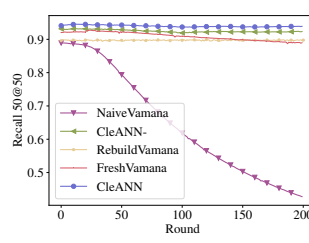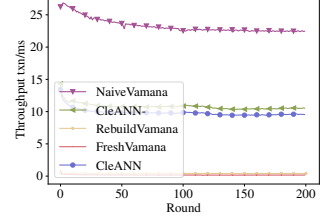
Figure 38: Average 10@10 recall vs. percentange of queries used for training for RedCaps and MS-SpaceV.

comparing the recall of the test queries of these training settings as well as the no-training setting.

The *in-distribution* training queries are generated as described in subsection 6.1. The *out-of-distribution* training queries are perturbed with a 1000x variance compared to the in-distribution training queries. Figure 37 presents the recalls from Search batches of three variants, all of which use tombstones for deleted points. The in-distribution and out-of-distribution variants insert new points with GuidedBridgeBuild. The *no training* variant does not perform GuidedBridgeBuild on search queries. We observe that using in-distribution training queries gives up to 18% higher recall during the workload compared to no training and up to 14% higher recall compared to training with out-of-distribution queries. This indicates that GuidedBridgeBuild adapts the index to the query workload.

We also study the amount of training needed to achieve these improvements. Figure 38 shows the average recall versus the percentage of in-distribution queries used for training on **Redcaps** and **MS-SpaceV**. The results on both datasets suggest that a small training sample is enough for GuidedBridgeBuild to add critical bridge edges that significantly improve the index. This suggests that some edges are disproportionately important for a graph to maintain a certain level of recall.

6.3.4 Ablation Study for Dynamic Cleaning

We present an ablation study experiment for the effect of adaptive on-the-fly neighborhood consolidation and semi-lazy memory cleaning. $C = 7$, $R = 64$, and $L = 64$ in this experiment.

We conduct the Sliding Window Batched Update experiment on **MS-SpaceV**, maintaining an index of size 500,000 and running the experiment for 100 rounds. We study **CleANN-** which only uses on-the-fly consolidation and semi-lazy cleaning and does not perform GuidedBridgeBuild. The memory available is initially set to

600,000 vectors, so that new data points cannot avoid reusing memory from semi-lazy memory cleaning. The results from **CleANN** with all proposed algorithms are also reported for comparison.

In Figure 39, we see that the recall of **FreshVamana** degrades slightly, likely due to the real-world distribution shift of the dataset. **CleANN-**'s recall is not only slightly higher but also more consistent across rounds as more updates happen thanks to the robustness benefits of our algorithms. The recall of **NaiveVamana** decreases significantly as the index becomes more contaminated by tombstones. GuidedBridgeBuild helps **CleANN** further improve upon **CleANN-** by improving the connections in the graph also in a query-aware manner.

Figure 40 shows that **CleANN-** has lower throughput than **NaiveVamana** due to having more work for on-the-fly consolidations. However, **CleANN-** is significantly more efficient than **RebuildVamana** and **FreshVamana**, which has prohibitive efficiency especially when the workload is update-heavy. These results suggest that our on-the-fly consolidation and memory cleaning methods contribute to both good recall and high efficiency by effectively fixing the graph around deleted nodes. **CleANN-** has slightly higher throughput than **CleANN** due to not incurring the cost of GuidedBridgeBuild.

6.3.5 Semi-lazy Memory Cleaning Hyperparameter Sensitivity

We present a micro-benchmark that studies the sensitivity of the cleaning threshold hyperparameter C by investigating how the performance of **CleANN** changes with different values of C. From Figures 41–47, we see that the recall increases with diminishing returns as the cleaning threshold C increases in all datasets, except for an anomaly in **Adversarial**. The ranges of recalls are also small (±3% at most). Higher values of C means that more incoming edges of a tombstone are actually removed instead of left to become a random edge. This generally corresponds to higher recall and lower throughput. For the datasets that we experiment on, the average recall increases by roughly 1% every time C doubles, starting from 3. **Yandex-tti** displays a different trend in efficiency: the higher C is, the better the efficiency is. This is possibly because of the lower update-to-search ratio or the maximum inner product metric that makes the index convergence behavior suffer more from random edges.

6.3.6 Random Edge Contamination Experiment

Given the same C, we study whether the technique of using graph nodes with existing incoming edges to represent a different data point as in edge $v_3 \rightarrow w_y$ in Figure 5 negatively affects the graph quality, measured with
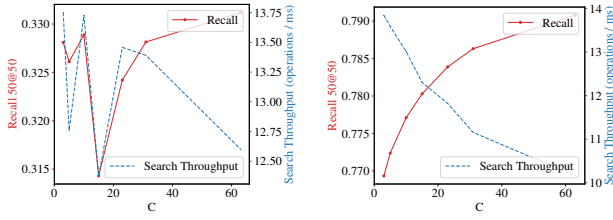
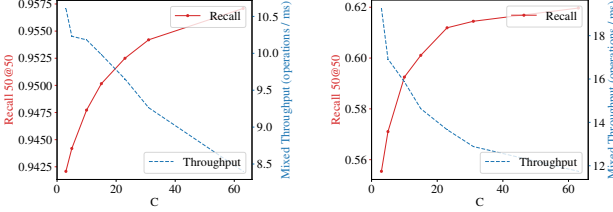**Figure 41: Average throughput and recall for Adversarial with index size 500k for different values of C.**

Figure 42: Average throughput and recall for GloVe with index size 500k for different values of C.

Figure 43: Average throughput and recall for HuffPost with index size 50k for different values of C.

Figure 44: Average throughput and recall for RedCaps with index size 500k for different values of C.

Figure 45: Average throughput and recall for Sift with index size 500k for different values of C.
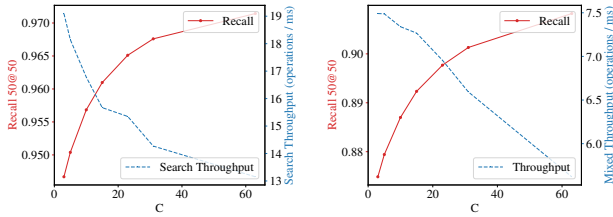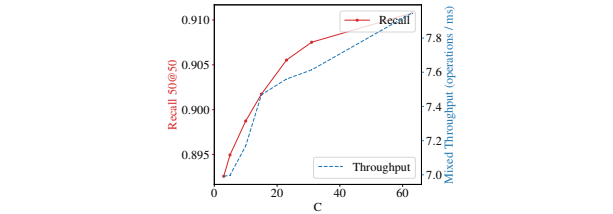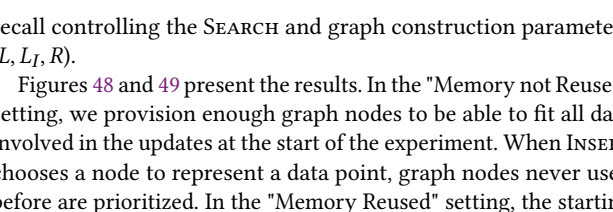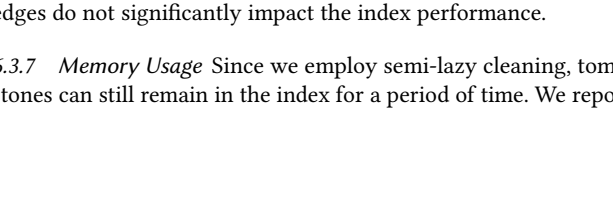

Figure 46: Average throughput and recall for MS-SpaceV with index size 500k for different values of C.

Figure 47: Average throughput and recall for Yandex-tti with index size 500k for different values of C.

recall controlling the SEARCH and graph construction parameters (L, L_I, R).

Figures 48 and 49 present the results. In the "Memory not Reused" setting, we provision enough graph nodes to be able to fit all data involved in the updates at the start of the experiment. When INSERT chooses a node to represent a data point, graph nodes never used before are prioritized. In the "Memory Reused" setting, the starting graph size is 1.2x the index size, and graph nodes used before are prioritized during an INSERT. We can see that the recall and update throughput differences are negligible. Hence, empirically, random edges do not significantly impact the index performance.

6.3.7 Memory Usage Since we employ semi-lazy cleaning, tombstones can still remain in the index for a period of time. We report
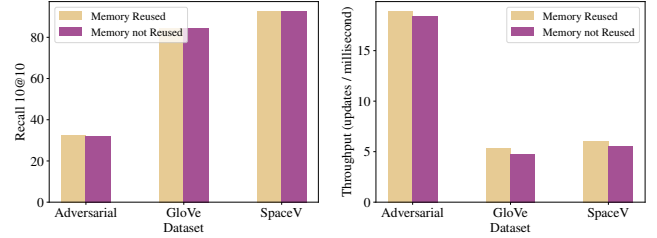

Figure 48: Average recall 10@10 on Adversarial, GloVe, and SpaceV with index size 500k over 100 rounds of the Sliding Window Batched Update experiment.

Figure 49: Average update throughput on Adversarial, GloVe, and SpaceV with index size 500k over 100 rounds of the Sliding Window Batched Update experiment.

Table 4: Peak Memory Overhead in the Sliding Window Batched Update setting.

Dataset	Overhead	Update-Search Ratio
Adversarial	90%	1
GloVe	5.4%	0.1
HuffPost	4.2%	0.1
RedCaps	15.2%	1
Sift	3.5%	0.1
SpaceV	13%	1
Yandex	4.9%	0.1

the **peak** memory overhead of CleANN over FreshVamana under the Sliding Window Batched Update setting with the respective update-search workload ratio under which these overheads are measured for our datasets. We set $C = 7$ in this experiment.

7 Related Work

In this section, we discuss previous works on ANN indexes.

Static ANN indexes have been extensively studied in the literature. Previous indexing methods can be roughly categorized into three main categories of techniques. Some works [5, 52] also combine multiple techniques for improved query performance. These approaches inherently struggle with the *boundary issue*: if a query points is close to a boundary of different partitions, indexed points in every partition need to be compared with the query. This is especially an issue in high dimensions since the number of possible spatial partition neighbors grows with the dimensionality.

Space-partition trees. Space partition indexes can be naturally extended to support ANNS. Given a query q, the index identifies the partition $\mathcal{P}(q)$ that q belongs to and potentially the partitions close to $\mathcal{P}(q)$. The indexed points in these identified partitions are further compared with q to find the nearest neighbors. Space partition indexes that have been applied to ANNS in this fashion include kd-trees [16, 23, 40], R-trees [26, 37], Random Projection (RP)-trees [9], Spill (SP)-trees [13, 30, 47], Voronoi Diagrams [25, 31], clustering [5], and Product Quantization [24]. These methods are also often combined with ideas from inverted indexes for improved performance.

Locality-sensitive hashing (LSH). Locality-sensitive hash functions hash points close to each other to hash values that are the same or close to each other with high probability. Indexed points in the same or similar hash buckets as the query point are compared with the query point. Many LSH functions are often used together to boost the success probability. LSH was first proposed for ANNS in [12, 18] and extensively studied subsequently [8, 10, 35].

LSH-based indexes have provable accuracy and efficiency guarantees, but do not attain the performance of graph-based indexes in practice [3].

Graph-based indexes. Some notable previous works for graph-based indexes include [11, 14, 20, 32, 33]. We introduce graph-based indexes in more detail in section 2 and refer the readers to [48] for a more comprehensive review.

Dynamic indexes. Fully-dynamic ANN indexes that maintain high recall under updates are less studied. Using different techniques for static ANNS mentioned above in the fully-dynamic setting induces different challenges than the ones addressed in this paper for graph-based ANN indexes. Naively applying static space-partition and LSH-based solutions in dynamic settings by inserting or deleting points into/from the partition or hash bucket creates partition/bucket imbalance problems. This can degrade the efficiency of the index and may exacerbate the partition/bucket boundary issues discussed above, which worsens the recall. **SPFresh** [50] uses dynamic rebalancing (based on space-partitioning) to solve this problem to obtain a dynamic version of the disk-oriented clustering-based index **SPANN** [5]. Dynamic rebalancing techniques are orthogonal to our methods, since we focus on graph-based techniques. A system like **SPFresh** that can combine a graph-based index with other algorithms could benefit from our methods. The existing dynamic graph-based indexes **FreshDiskANN**, **DEG**, and **LSH-APG**, as well as graph-based entries in the NeurIPS 2023 streaming ANN computation [1], either use expensive global updates or suffer from query quality degradation.

Recent works **DIGRA** [22] and **RangePQ** [51] propose algorithms for dynamic ANNS supporting range queries, leveraging tree structures. Their update algorithms focus on maintaining the tree structures themselves. Our work focuses instead on an efficient and robust solution for updating the graphs in graph-based ANNS.

The concurrent and independent work **IP-DiskANN** [49] focuses on efficiently supporting Delete queries in place. When a data point p is deleted, **IP-DiskANN** searches for p and heuristically selects in-neighbors of v_p visited during the search to absorb some other nodes close to p into their neighborhoods. On the other hand, **CleANN** does consolidation in subsequent operations and is informed by the query workload, while also providing methods to improve robustness. It would be interesting to compare the two solutions in future work.

8 Conclusion

We presented adaptive, robust, and efficient methods to improve the performance of graph-based ANN indexes in the setting of full dynamism. We designed the **CleANN** system, which implements our methods on top of **Vamana**. Our system avoids expensive global updates, adapts to the workload, and is the first concurrent graph-based index to support full dynamism efficiently. Future research opportunities include combining our methods with other graph-based ANN approaches, adapting machine learning techniques from learned indexes to improve performance, as well as theoretically analyzing the performance and robustness of dynamic ANNS.

References

[1] [n. d.]. big-ann-benchmarks/neurips23/streaming at main · harsha-simhadri/big-ann-benchmarks — github.com. https://github.com/harsha-simhadri/big-ann-benchmarks/tree/main/neurips23/streaming. [Accessed 01-10-2024].

[2] [n. d.]. YouTube for Press. https://blog.youtube/press/ Accessed on September 24, 2024.

[3] Martin Aumüller, Erik Bernhardsson, and Alexander Faithfull. 2018. ANN-Benchmarks: A Benchmarking Tool for Approximate Nearest Neighbor Algorithms. arXiv:1807.05614 [cs.IR] https://arxiv.org/abs/1807.05614

[4] Dimitry Baranchuk and Artem Babenko. [n. d.]. Yandex — research.yandex.com. https://research.yandex.com/datasets/text-to-image-dataset-for-billion-scale-similarity-search. [Accessed 30-07-2024].

[5] Qi Chen, Bing Zhao, Haidong Wang, Mingqin Li, Chuanjie Liu, Zengzhong Li, Mao Yang, and Jingdong Wang. 2021. SPANN: Highly-efficient Billion-scale Approximate Nearest Neighbor Search. CoRR abs/2111.08566 (2021). arXiv:2111.08566 https://arxiv.org/abs/2111.08566

[6] Yewang Chen, Shengyu Tang, Nizar Bouguila, Cheng Wang, Jixiang Du, and HaiLin Li. 2018. A fast clustering algorithm based on pruning unnecessary distance computations in DBSCAN for high-dimensional data. Pattern Recognition 83 (2018), 375–387.

[7] SpaceV Contributors. 2023. SPTAG/datasets/SPACEV1B at main · microsoft/SPTAG — github.com. https://github.com/microsoft/SPTAG/tree/main/datasets/SPACEV1B. [Accessed 30-07-2024].

[8] Anirban Dasgupta, Ravi Kumar, and Tamas Sarlos. 2011. Fast locality-sensitive hashing. In Proceedings of the 17th ACM SIGKDD International Conference on Knowledge Discovery and Data Mining (San Diego, California, USA) (KDD '11). Association for Computing Machinery, New York, NY, USA, 1073–1081. https://doi.org/10.1145/2020408.2020578

[9] Sanjoy Dasgupta and Kaushik Sinha. 2015. Randomized Partition Trees for Nearest Neighbor Search. Algorithmica 72, 1 (01 May 2015), 237–263. https://doi.org/10.1007/s00453-014-9885-5

[10] Mayur Datar, Nicole Immorlica, Piotr Indyk, and Vahab S. Mirrokni. 2004. Locality-sensitive hashing scheme based on p-stable distributions. In Proceedings of the Twentieth Annual Symposium on Computational Geometry (Brooklyn, New York, USA) (SCG '04). Association for Computing Machinery, New York, NY, USA, 253–262. https://doi.org/10.1145/997817.997857

[11] Cong Fu, Chao Xiang, Changxu Wang, and Deng Cai. 2019. Fast approximate nearest neighbor search with the navigating spreading-out graph. Proc. VLDB Endow. 12, 5 (jan 2019), 461–474. https://doi.org/10.14778/3303753.3303754

[12] Aristides Gionis, Piotr Indyk, and Rajeev Motwani. 1999. Similarity Search in High Dimensions via Hashing. In Proceedings of the 25th International Conference on Very Large Data Bases (VLDB '99). Morgan Kaufmann Publishers Inc., San Francisco, CA, USA, 518–529.

[13] Ruiqi Guo, Philip Sun, Erik Lindgren, Quan Geng, David Simcha, Felix Chern, and Sanjiv Kumar. 2020. Accelerating Large-Scale Inference with Anisotropic Vector Quantization. In International Conference on Machine Learning. https://arxiv.org/abs/1908.10396

[14] Ben Harwood and Tom Drummond. 2016. FANNG: Fast Approximate Nearest Neighbour Graphs. In 2016 IEEE Conference on Computer Vision and Pattern Recognition (CVPR). 5713–5722. https://doi.org/10.1109/CVPR.2016.616

[15] Nico Hezel, Uwe Kai Barthel, Konstantin Schall, and Klaus Jung. 2023. Fast Approximate nearest neighbor search with the Dynamic Exploration Graph using continuous refinement. CoRR abs/2307.10479 (2023).

[16] Linjia Hu, Saeid Nooshabadi, and Majid Ahmadi. 2015. Massively parallel KD-tree construction and nearest neighbor search algorithms. In 2015 IEEE International Symposium on Circuits and Systems (ISCAS). 2752–2755. https://doi.org/10.1109/ISCAS.2015.7169256

[17] HuffPost, Rishabh Misra, and Ziyu Zhang. 2024. Embedded HuffPost New Category Dataset.

[18] Piotr Indyk and Rajeev Motwani. 1998. Approximate nearest neighbors: towards removing the curse of dimensionality. In Proceedings of the Thirtieth Annual ACM Symposium on Theory of Computing (Dallas, Texas, USA) (STOC '98). Association for Computing Machinery, New York, NY, USA, 604–613. https://doi.org/10.1145/276698.276876

[19] Masajiro Iwasaki and Daisuke Miyazaki. 2018. Optimization of Indexing Based on k-Nearest Neighbor Graph for Proximity Search in High-dimensional Data. arXiv:1810.07355 [cs.DB] https://arxiv.org/abs/1810.07355

[20] Suhas Jayaram Subramanya, Fnu Devvrit, Harsha Vardhan Simhadri, Ravishankar Krishnawamy, and Rohan Kadekodi. 2019. DiskANN: Fast Accurate Billion-point

Nearest Neighbor Search on a Single Node. In *Advances in Neural Information Processing Systems*, H. Wallach, H. Larochelle, A. Beygelzimer, F. d'Alché-Buc, E. Fox, and R. Garnett (Eds.), Vol. 32. Curran Associates, Inc. https://proceedings.neurips.cc/paper_files/paper/2019/file/09853c7fb1d3f8ee67a61b6bf4a7f8e6-Paper.pdf

[21] Hervé Jégou, Matthijs Douze, and Cordelia Schmid. 2011. Product Quantization for Nearest Neighbor Search. *IEEE Transactions on Pattern Analysis and Machine Intelligence* 33, 1 (Jan. 2011), 117–128. https://doi.org/10.1109/TPAMI.2010.57

[22] Mengxu Jiang, Zhi Yang, Fangyuan Zhang, Guanhao Hou, Jieming Shi, Wenchao Zhou, Feifei Li, and Sibo Wang. 2025. DIGRA: A Dynamic Graph Indexing for Approximate Nearest Neighbor Search with Range Filter. *Proc. ACM Manag. Data* 3, 3, Article 148 (June 2025), 26 pages. https://doi.org/10.1145/3725399

[23] Jaemin Jo, Jinwook Seo, and Jean-Daniel Fekete. 2017. A progressive k-d tree for approximate k-nearest neighbors. In *2017 IEEE Workshop on Data Systems for Interactive Analysis (DSIA)*. 1–5. https://doi.org/10.1109/DSIA.2017.8339084

[24] Herve Jégou, Matthijs Douze, and Cordelia Schmid. 2011. Product Quantization for Nearest Neighbor Search. *IEEE Transactions on Pattern Analysis and Machine Intelligence* 33, 1 (2011), 117–128. https://doi.org/10.1109/TPAMI.2010.57

[25] Mohammad Kolahdouzan and Cyrus Shahabi. 2004. Voronoi-based K nearest neighbor search for spatial network databases. In *Proceedings of the Thirtieth International Conference on Very Large Data Bases - Volume 30* (Toronto, Canada) *(VLDB '04)*. VLDB Endowment, 840–851.

[26] J. Kuan and P. Lewis. 1997. Fast k nearest neighbour search for R-tree family. In *Proceedings of ICICS, 1997 International Conference on Information, Communications and Signal Processing. Theme: Trends in Information Systems Engineering and Wireless Multimedia Communications (Cat.*, Vol. 2. 924–928 vol.2. https://doi.org/10.1109/ICICS.1997.652114

[27] Patrick Lewis, Ethan Perez, Aleksandra Piktus, Fabio Petroni, Vladimir Karpukhin, Naman Goyal, Heinrich Küttler, Mike Lewis, Wen tau Yih, Tim Rocktäschel, Sebastian Riedel, and Douwe Kiela. 2021. Retrieval-Augmented Generation for Knowledge-Intensive NLP Tasks. arXiv:2005.11401 [cs.CL] https://arxiv.org/abs/2005.11401

[28] Jie Li, Haifeng Liu, Chuanghua Gui, Jianyu Chen, Zhenyuan Ni, Ning Wang, and Yuan Chen. 2018. The design and implementation of a real time visual search system on JD E-commerce platform. In *Proceedings of the 19th International Middleware Conference Industry*. 9–16.

[29] Sen Li, Fuyu Lv, Taiwei Jin, Guli Lin, Keping Yang, Xiaoyi Zeng, Xiao-Ming Wu, and Qianli Ma. 2021. Embedding-based product retrieval in taobao search. In *Proceedings of the 27th ACM SIGKDD Conference on Knowledge Discovery & Data Mining*. 3181–3189.

[30] Ting Liu, Andrew Moore, Ke Yang, and Alexander Gray. 2004. An Investigation of Practical Approximate Nearest Neighbor Algorithms. In *Advances in Neural Information Processing Systems*, L. Saul, Y. Weiss, and L. Bottou (Eds.), Vol. 17. MIT Press. https://proceedings.neurips.cc/paper_files/paper/2004/file/1102a326d5f7c9e04fc3c89d0ede88c9-Paper.pdf

[31] Kejing Lu, Mineichi Kudo, Chuan Xiao, and Yoshiharu Ishikawa. 2021. HVS: hierarchical graph structure based on voronoi diagrams for solving approximate nearest neighbor search. *Proc. VLDB Endow.* 15, 2 (oct 2021), 246–258. https://doi.org/10.14778/3489496.3489506

[32] Yury Malkov, Alexander Ponomarenko, Andrey Logvinov, and Vladimir Krylov. 2014. Approximate nearest neighbor algorithm based on navigable small world graphs. *Information Systems* 45 (2014), 61–68. https://doi.org/10.1016/j.is.2013.10.006

[33] Yu A. Malkov and D. A. Yashunin. 2020. Efficient and Robust Approximate Nearest Neighbor Search Using Hierarchical Navigable Small World Graphs. *IEEE Transactions on Pattern Analysis and Machine Intelligence* 42, 4 (2020), 824–836. https://doi.org/10.1109/TPAMI.2018.2889473

[34] Magdalen Dobson Manohar, Zheqi Shen, Guy Blelloch, Laxman Dhulipala, Yan Gu, Harsha Vardhan Simhadri, and Yihan Sun. 2024. ParlayANN: Scalable and Deterministic Parallel Graph-Based Approximate Nearest Neighbor Search Algorithms. In *Proceedings of the 29th ACM SIGPLAN Annual Symposium on Principles and Practice of Parallel Programming* (Edinburgh, United Kingdom) *(PPoPP '24)*. Association for Computing Machinery, New York, NY, USA, 270–285. https://doi.org/10.1145/3627535.3638475

[35] Rajeev Motwani, Assaf Naor, and Rina Panigrahi. 2006. Lower bounds on locality sensitive hashing. In *Proceedings of the Twenty-Second Annual Symposium on Computational Geometry* (Sedona, Arizona, USA) *(SCG '06)*. Association for Computing Machinery, New York, NY, USA, 154–157. https://doi.org/10.1145/1137856.1137881

[36] Felix Ocker, Daniel Tanneberg, Julian Eggert, and Michael Gienger. 2024. Tulip Agent–Enabling LLM-Based Agents to Solve Tasks Using Large Tool Libraries. *arXiv preprint arXiv:2407.21778* (2024).

[37] Apostolos Papadopoulos and Yannis Manolopoulos. 1997. Performance of nearest neighbor queries in R-trees. In *Database Theory — ICDT '97*, Foto Afrati and Phokion Kolaitis (Eds.). Springer Berlin Heidelberg, Berlin, Heidelberg, 394–408.

[38] Jeffrey Pennington, Richard Socher, and Christopher Manning. 2014. GloVe: Global Vectors for Word Representation. In *Proceedings of the 2014 Conference on Empirical Methods in Natural Language Processing (EMNLP)*, Alessandro Moschitti, Bo Pang, and Walter Daelemans (Eds.). Association for Computational

Linguistics, Doha, Qatar, 1532–1543. https://doi.org/10.3115/v1/D14-1162

[39] Erion Plaku and Lydia E Kavraki. 2008. Quantitative analysis of nearest-neighbors search in high-dimensional sampling-based motion planning. In *Algorithmic Foundation of Robotics VII: Selected Contributions of the Seventh International Workshop on the Algorithmic Foundations of Robotics*. Springer, 3–18.

[40] Parikshit Ram and Kaushik Sinha. 2019. Revisiting kd-tree for Nearest Neighbor Search. In *Proceedings of the 25th ACM SIGKDD International Conference on Knowledge Discovery & Data Mining* (Anchorage, AK, USA) *(KDD '19)*. Association for Computing Machinery, New York, NY, USA, 1378–1388. https://doi.org/10.1145/3292500.3330875

[41] Reddit, Karan Desai, Gaurav Kaul, Zubin Aysola, Justin Johnson, Joshua Engels, Ziyu Zhang, and OpenAI (United States). 2024. CLIP-Embedded RedCaps Text-Image Dataset.

[42] Aviad Rubinstein. 2018. Hardness of approximate nearest neighbor search. In *Proceedings of the 50th Annual ACM SIGACT Symposium on Theory of Computing* (Los Angeles, CA, USA) *(STOC 2018)*. Association for Computing Machinery, New York, NY, USA, 1260–1268. https://doi.org/10.1145/3188745.3188916

[43] Maying Shen, Xinghao Jiang, and Tanfeng Sun. 2018. Anomaly detection based on nearest neighbor search with locality-sensitive B-tree. *Neurocomputing* 289 (2018), 55–67.

[44] Harsha Vardhan Simhadri, Ravishankar Krishnaswamy, Gopal Srinivasa, Suhas Jayaram Subramanya, Andrija Antonijevic, Dax Pryce, David Kaczynski, Shane Williams, Siddarth Gollapudi, Varun Sivashankar, Neel Karia, Aditi Singh, Shikhar Jaiswal, Neelam Mahapatro, Philip Adams, Bryan Tower, and Yash Patel. 2023. DiskANN: Graph-structured Indices for Scalable, Fast, Fresh and Filtered Approximate Nearest Neighbor Search. https://github.com/Microsoft/DiskANN

[45] Aditi Singh, Suhas Jayaram Subramanya, Ravishankar Krishnaswamy, and Harsha Vardhan Simhadri. 2021. FreshDiskANN: A Fast and Accurate Graph-Based ANN Index for Streaming Similarity Search. arXiv:2105.09613 [cs.IR] https://arxiv.org/abs/2105.09613

[46] Ján Suchal and Pavol Návrat. 2010. Full text search engine as scalable k-nearest neighbor recommendation system. In *Artificial Intelligence in Theory and Practice III: Third IFIP TC 12 International Conference on Artificial Intelligence, IFIP AI 2010, Held as Part of WCC 2010, Brisbane, Australia, September 20-23, 2010. Proceedings 3*. Springer, 165–173.

[47] Philip Sun, David Simcha, Dave Dopson, Ruiqi Guo, and Sanjiv Kumar. 2023. SOAR: Improved Indexing for Approximate Nearest Neighbor Search. In *Neural Information Processing Systems*. https://arxiv.org/abs/2404.00774

[48] Mengzhao Wang, Xiaoliang Xu, Qiang Yue, and Yuxiang Wang. 2021. A comprehensive survey and experimental comparison of graph-based approximate nearest neighbor search. *Proc. VLDB Endow.* 14, 11 (jul 2021), 1964–1978. https://doi.org/10.14778/3476249.3476255

[49] Haike Xu, Magdalen Dobson Manohar, Philip A. Bernstein, Badrish Chandramouli, Richard Wen, and Harsha Vardhan Simhadri. 2025. In-Place Updates of a Graph Index for Streaming Approximate Nearest Neighbor Search. arXiv:2502.13826 [cs.IR] https://arxiv.org/abs/2502.13826

[50] Yuming Xu, Hengyu Liang, Jin Li, Shuotao Xu, Qi Chen, Qianxi Zhang, Cheng Li, Ziyue Yang, Fan Yang, Yuqing Yang, Peng Cheng, and Mao Yang. 2023. SPFresh: Incremental In-Place Update for Billion-Scale Vector Search. In *Proceedings of the 29th Symposium on Operating Systems Principles* (Koblenz, Germany) *(SOSP '23)*. Association for Computing Machinery, New York, NY, USA, 545–561. https://doi.org/10.1145/3600006.3613166

[51] Fangyuan Zhang, Mengxu Jiang, Guanhao Hou, Jieming Shi, Hua Fan, Wenchao Zhou, Feifei Li, and Sibo Wang. 2025. Efficient Dynamic Indexing for Range Filtered Approximate Nearest Neighbor Search. *Proc. ACM Manag. Data* 3, 3, Article 152 (June 2025), 26 pages. https://doi.org/10.1145/3725401

[52] Xi Zhao, Yao Tian, Kai Huang, Bolong Zheng, and Xiaofang Zhou. 2023. Towards Efficient Index Construction and Approximate Nearest Neighbor Search in High-Dimensional Spaces. *Proc. VLDB Endow.* 16, 8 (apr 2023), 1979–1991. https://doi.org/10.14778/3594512.3594527